Taylor & Francis
Taylor & Francis Group

Critical Reviews in Toxicology

ISSN: 1040-8444 (Print) 1547-6898 (Online) Journal homepage: https://www.tandfonline.com/loi/itxc20

Advances in detection of hazardous organophosphorus compounds using organophosphorus hydrolase based biosensors

Monika Jain, Priyanka Yadav, Abhijeet Joshi & Prashant Kodgire

To cite this article: Monika Jain, Priyanka Yadav, Abhijeet Joshi & Prashant Kodgire (2019): Advances in detection of hazardous organophosphorus compounds using organophosphorus hydrolase based biosensors, Critical Reviews in Toxicology, DOI: 10.1080/10408444.2019.1626800

To link to this article: https://doi.org/10.1080/10408444.2019.1626800

Published online: 03 Jul 2019.

CRITICAL REVIEWS IN TOXICOLOGY
https://doi.org/10.1080/10408444.2019.1626800

Taylor & Francis
Taylor & Francis Group

REVIEW ARTICLE

Advances in detection of hazardous organophosphorus compounds using organophosphorus hydrolase based biosensors

Monika Jain, Priyanka Yadav, Abhijeet Joshi and Prashant Kodgire

Discipline of Biosciences and Biomedical Engineering, Indian Institute of Technology, Indore, India

ABSTRACT

Agricultural advancements focusing on increasing crop production have led to excessive usage of insecticides and pesticides, resulting in leaching and accumulation of these highly toxic chemicals in soil, water, and the food-chain. Organophosphorus (OP) compounds are the most commonly used insecticides and pesticides, which cause a wide range of long-lasting and life-threatening conditions. Due to the acute toxicity and long-term side effects of OP compounds, their timely, on-the-spot and rapid detection has gained importance, for efficient healthcare management. In this respect, several OP degrading enzymes have gained the spotlight in developing the enzyme-based biosensors, owing to their high activity and broad specificity. Among these enzymes, organophosphorus hydrolase (OPH) has emerged as a promising candidate for the detection of OP compounds, due to its ability to act on a broad range of substrates having a variety of bonds, like P—F, P—O, P—S, and P—CN. Various techniques employing OPH in free/immobilized/conjugated forms into sensing devices were reported to accurately detect OP compounds. The transduction mechanisms of bio-sensing are electrochemical, optical as well as novel methods like magnetoelastic/surface plasmon resonance. Furthermore, to improve the detection limits and sensitivity, nanoparticles and quantum dots are often employed in conjunction with OPH. Here, we highlight the recent advances in sensing OP compounds using OPH based biosensors, compare specifications of sensing methods, and evaluate the influence of different materials used in developing sensors. This review will also enable researchers to design and configure highly sensitive and accurate sensing systems, leading to the development of point-of-care devices for real-time analysis.

ARTICLE HISTORY
Received 1 January 2019
Revised 14 May 2019
Accepted 16 May 2019

KEYWORDS
Biosensor; organophosphorus (OP) compounds; acetylcholinesterase (AChE); organophosphorus hydrolase (OPH); nerve agents

Table of contents

Introduction

In recent times, increasing population has led to higher demand for the food supplies, thus necessitating increased yield from the existing arable land, and expanding the types and quantity of agricultural produce. A direct consequence of the massive agricultural expansion is increased use of pesticides in order to enhance the productivity of the crops.

CONTACT Prashant Kodgire pkodgire@iiti.ac.in; Abhijeet Joshi abhijeet.joshi@iiti.ac.in Discipline of Biosciences and Biomedical Engineering, Indian Institute of Technology Indore, IIT Indore, Khandwa Road, Simrol, Indore 453552, India

Incidentally, over 5.6 billion pounds of pesticides are used globally every year (Donaldson et al. 1997). The most well-known commercial pesticides are classified broadly into three categories: organochlorines, carbamates, and organophosphates. Of these, organophosphates – also called phosphotriesters due to the presence of three phosphodiester bonds (Figure 1) (Barr et al. 2004), are of substantial interest due to their low-cost of synthesis and high efficacy. Strikingly, OP-based compounds today constitute anywhere between 33% of available pesticides in the developed countries and 50–60% in the developing countries (Atwood and Paisley-Jones 2017). Incidentally, trace amount of these compounds exhibit toxicity when absorbed through the skin, ingested or inhaled. In fact, World Health Organization reports show that around 200 000 people suffer annually from pesticide-related poisoning due to the direct or indirect exposure to organophosphorus compounds (OPs) (Theriot and Grunden 2011). For researchers in medical and environmental sciences, the use of OPs has been of a particular concern due to its lower biodegradability compared to the newer pesticides, as well as their tendency to block the active site of important enzymes in neurons, such as acetylcholinesterase (AChE), which breaks down and removes acetylcholine from the nerve synapse. The inability to break down acetylcholine results in neurological problems, such as convulsions, tremors, and even death (Zimmer et al. 1998). Although the OP poisoning is treatable using a combination of atropine and pralidoxime (Eddleston et al. 2008), such medication has several side effects (Headley 1982) and is not as effective in patients with prolonged exposure due to a phenomenon known as the aging effect, in which a non-enzymatic loss of alkyl chain from the phosphate group in the OP compound renders the inhibited/blocked AChE into a non-reactivatable form (Masson et al. 2010). Strikingly, poisoning by the OPs has a high rate of mortality (Eddleston 2000) that exceeds the normal expectations for exposure to toxic chemicals, such as mercury, cyanide, and cadmium. These higher mortality rates are a cause of concern for healthcare professionals to this day (Muley et al. 2014), necessitating measures to facilitate a convenient and accurate detection of OPs in human samples as well as environment.

In this review, we attempt to highlight the detection of these compounds using biosensors with a focus on mechanisms of action, development of novel detection methods and analysis of the capabilities of reported sensors. We provide up-to-date details of the developed biosensors and insights on the most suited sensing assay for OPs.

Organophosphorus compounds (OPs) and their effects

OPs were introduced as pesticides mainly in the 1950s and 1960s, and are widely used as insecticides, herbicides, nematicides as well as acaricides. Several derivatives of OPs are commercially marketed and they show prolonged half-life in the soil. For example, parathion shows half-life in the soil for 30–180 d, whereas another OP compound, coumaphos, shows half-life in the soil for 24–1400 d (Singh and Walker 2006).

Continuous or long exposure of the OPs leads to the deposition of these compounds at the depot site, from where they are uninterruptedly released into the blood. Subsequently, from blood, they reach the nervous system where one of their targets is the AChE enzyme (Masson et al. 1998). Figure 2 represents the bioavailability and metabolism of OPs in the human body. Once a person is exposed to the OPs, these compounds may get deposited into the site like liver, kidney, muscles, adipose tissue or they may get distributed to the central nervous system *via* blood circulation. The amount that remains in the blood is eliminated out *via* urine, expired air or in feces (Masson et al. 1998; Paraíba et al. 2009). In addition to AChE, these compounds target some

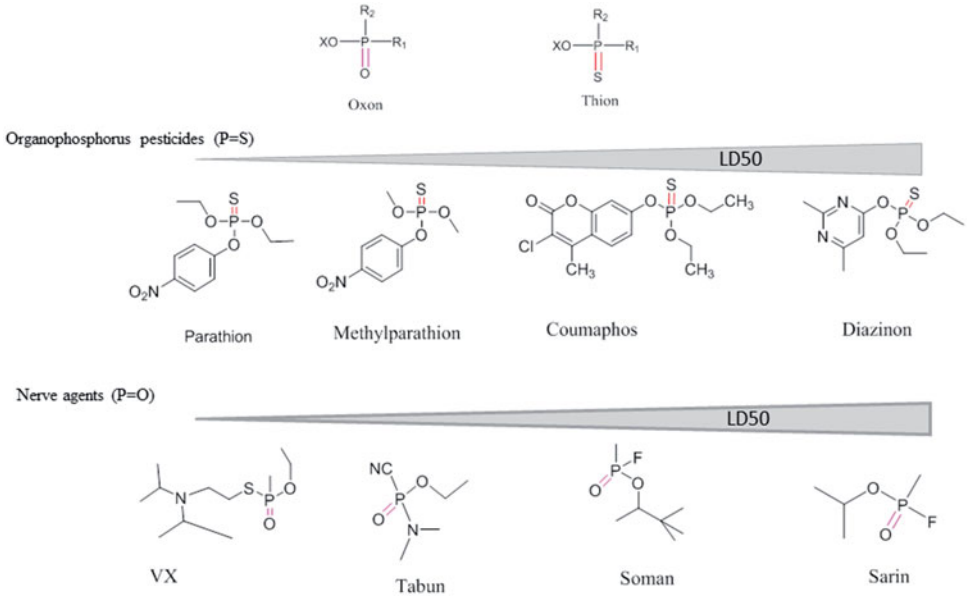

Figure 1. General structure of OPs: R_1 and R_2 are aryl or alkyl groups that are either bonded to phosphorus *via* the oxygen or sulfur link or they are directly bonded to the phosphorus. X group attached to the phosphorus may be an aromatic group, halogen, aliphatic or heterologous cyclic group (Vilanova and Sogorb 1999; Barr et al. 2004).

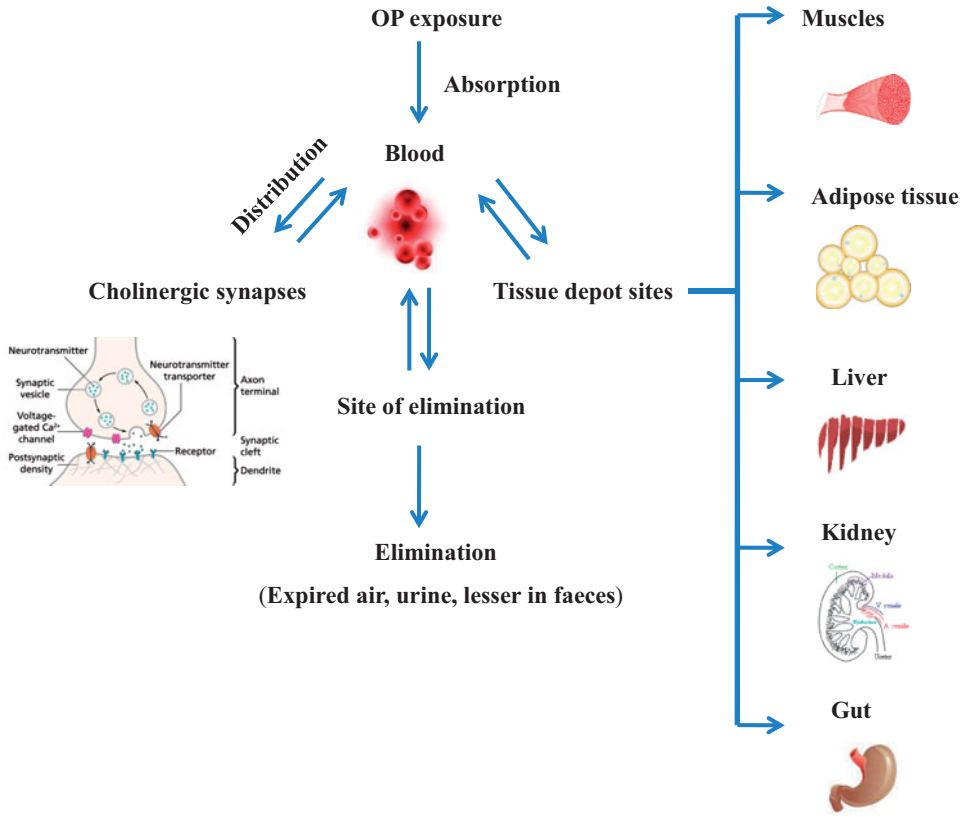

Figure 2. Representation of the bioavailability and metabolism of OPs in the human body (Masson et al. 1998); (Paraíba et al. 2009): When a person accidentally or deliberately inhales, ingests or absorbs the OPs, it reaches either to its depot site like muscles, adipose tissue, liver, kidney, or gut or it may get distributed to the central nervous system through the blood circulation. The amount that remains in the blood is eliminated out *via* urine, expired air or in feces.

important enzymes like lipases and esterases that are crucial for the proper functioning of the human body.

Effect of OPs on AChE

AChE is an enzyme that catalyzes the hydrolysis of acetylcholine, a neurotransmitter that is involved in the transfer of nerve impulses to the effector cells at cholinergic, synaptic as well as neuro-muscular junctions (Figure 3(A)). Several studies have indicated that OPs mainly interact with the AChE active sites (residues Ser203, His447, and Glu334) through phosphorylation (Figure 3(B)), wherein a covalent bond between the central phosphorus atom of the ligand and an oxygen atom from the side chain of a serine residue is formed (Guo et al. 2006). In some cases, the reaction may continue further, causing the loss of an alkyl chain from the resulting phosphyl alkoxy substituent. This process is known as "aging" and prevents reactivation of AChE by the conventional therapy. Once AChE is inactivated, the enzyme loses its ability to hydrolyze acetylcholine, and the build-up of acetylcholine causes continuous stimulation of muscle or nerve fibers, resulting in exhaustion and/or tetany (Fukuto 1990). A schematic of the inhibition mechanism of AChE by paraoxon a well-known OP compound, is given in Figure 3(A). The aging process is caused by a dealkylation reaction (Barak et al. 1997) which causes the resultant adduct to be remarkably unreactive and hence results in the irreversible inactivation of AChE.

Quinn et al. proposed that the inherent unreactivity and irreversibility caused by the aging is attributed to the structural similarity of the aged adducts to the tetrahedral intermediate of AChE in the deacylation stage of catalysis (Quinn et al. 2017). It is speculated that the overstimulation of glutamate receptors caused by inhibition of AChE as well as non-AChE targets, leads to convulsions, cardiac collapse, and respiratory arrest, whereas massive histamine release may be responsible for anaphylactic shocks (Duysen et al. 2001). Thus, OPs target not only AChE but also other enzymes, which make them a severe health hazard and thus warrants urgent development of detection as well as remediation techniques (Duysen et al. 2001).

Organophosphorus compounds induced neuropathy

OP-induced delayed polyneuropathy is also a severe toxic effect of OPs exerted on the central nervous system and peripheral nervous system. The root cause of this neuropathy is the modification and phosphorylation of the neuropathy target esterase enzyme in the central nervous system. An increase in autophosphorylation has been observed in the calmodulin kinases due to the presence of OPs. This increases the phosphorylation of cytoskeletal proteins, such as myelin basic protein, α and β tubulin, neurofilament protein, microtubule-associated protein-2. Consequently, the transport rate of cytoskeletal protein is decreased down the axon compared to their entry rate resulting in their accumulation in the distal part of the axon. Thus, the delayed OP-induced polyneuropathy is marked by bulging in the axons of the central and

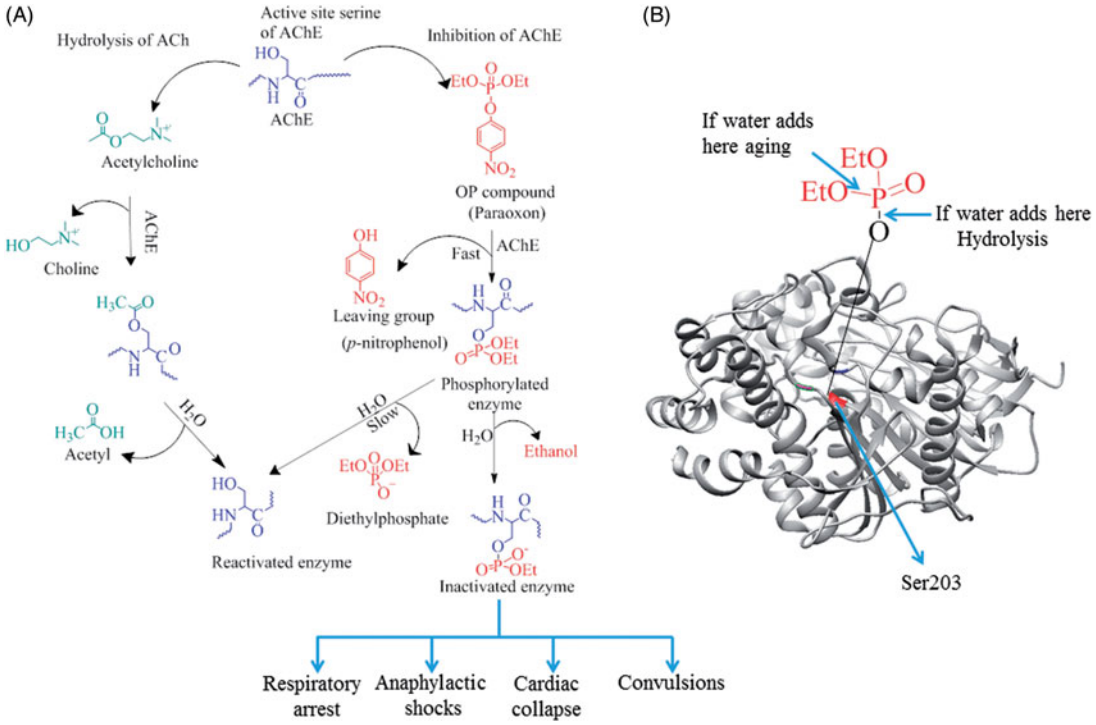

Figure 3. (A) Inhibition of AChE by OPs (Raushel 2002; Barr et al. 2004): OPs bind to the hydroxyl group of the serine at active site to form the phosphorylated enzyme resulting in the accumulation of the Acetylcholine at the synapses because inactivated AChE is unable to hydrolyze acetylcholine. (B) Structure of human Acetylcholinesterase (PDB ID-4PQE).

peripheral nervous system with subsequent ataxia and paralysis (Abou-Donia 1995).

Additionally, OPs shows other cellular effects such as inhibition of catecholamine released in chromaffin cells, inhibition of brain of rats, alteration in the level of inositol phosphate in SH-SY5Y cells, inhibition of pig kidney Na^+/K^+ ATPase, alteration in the hindbrain of the chicken on the ganglioside profile, change in the fluidity of the membrane, and biochemical changes in the bovine chromaffin cell's mitochondria (Vilanova and Sogorb 1999; Sogorb and Vilanova 2002).

Organophosphorus hydrolase (OPH)

The hazardous OPs can be degraded naturally by enzymes, such as organophosphorus hydrolase (OPH) and methyl parathion hydrolase (MPH), into less toxic or nontoxic compounds like *p*-nitrophenol and diethyl phosphate (Orbulescu et al. 2006). OPH enzyme is isolated from soil microorganisms, such as *Pseudomonas diminuta* and *Flavobacterium* species. OPH is also known as phosphotriesterase (PTE), organophosphorus degrading enzyme, and parathion hydrolase. This enzyme is encoded by the phosphate degrading gene (*opd)* located on the extrachromosomal plasmid (Raushel 2002). It has a broad substrate specificity and is able to hydrolyze P—O, P—CN, P—F, and P—S bonds (Orbulescu et al. 2006). On hydrolysis of the bond, it generates two protons and one alcohol, which are often electroactive or chromophoric (Mulchandani, Chen, Mulchandani, Wang, Rogers 2001; Theriot and Grunden 2011). Thus, OPH can be combined with pH electrode or a field-effect transistor based pH indicator to measure the protons produced or optical transducer to quantify the amount of *p*-nitrophenol produced during hydrolysis based on the chromophore produced (Mulchandani, Chen, Mulchandani, Wang, Rogers 2001). OPH has been proved to be an effective biocatalyst for hydrolysis of OPs, owing to which it has been considered for the purpose of detection and/or remediation of OPs (Figure 4(A)) (Jacquet et al. 2016).

Structure of OPH

PTE/OPH, a homodimer metalloprotein, is a member of superfamily amidohydrolase. It utilizes a divalent ion, such as Co^{2+}, Zn^{2+}, Mg^{2+}, Ca^{2+}, and Fe^{2+} etc., for the nucleophilic attack by activating the hydrolytic water molecules (Ghanem and Raushel 2005). With respect to the normal activity, enzymes supplemented with these ions show 121, 86, 81, 74, and 48% activity, respectively. The high-resolution X-ray structure showed that the protein folds into αβ barrel motif also known as TIM Barrel (Raushel 2002). OPH adopts TIM barrel fold where the active site is located at the C terminal of the β barrel (Ghanem and Raushel 2005). Two Zn^{2+} are bound to the histidine residues at the binuclear metallic center. One zinc cation is bound to two histidine residues, H201 from β strand 5 and H206 from β strand 6. Another zinc cation is bound to two histidine residues (H55 and H57) and one aspartic acid (D301) (Ghanem and Raushel 2005; Bigley and Raushel 2013). Carboxylated lysine from β strand 4 and hydroxide ion form the bridge between the two cations (Bigley and Raushel 2013).

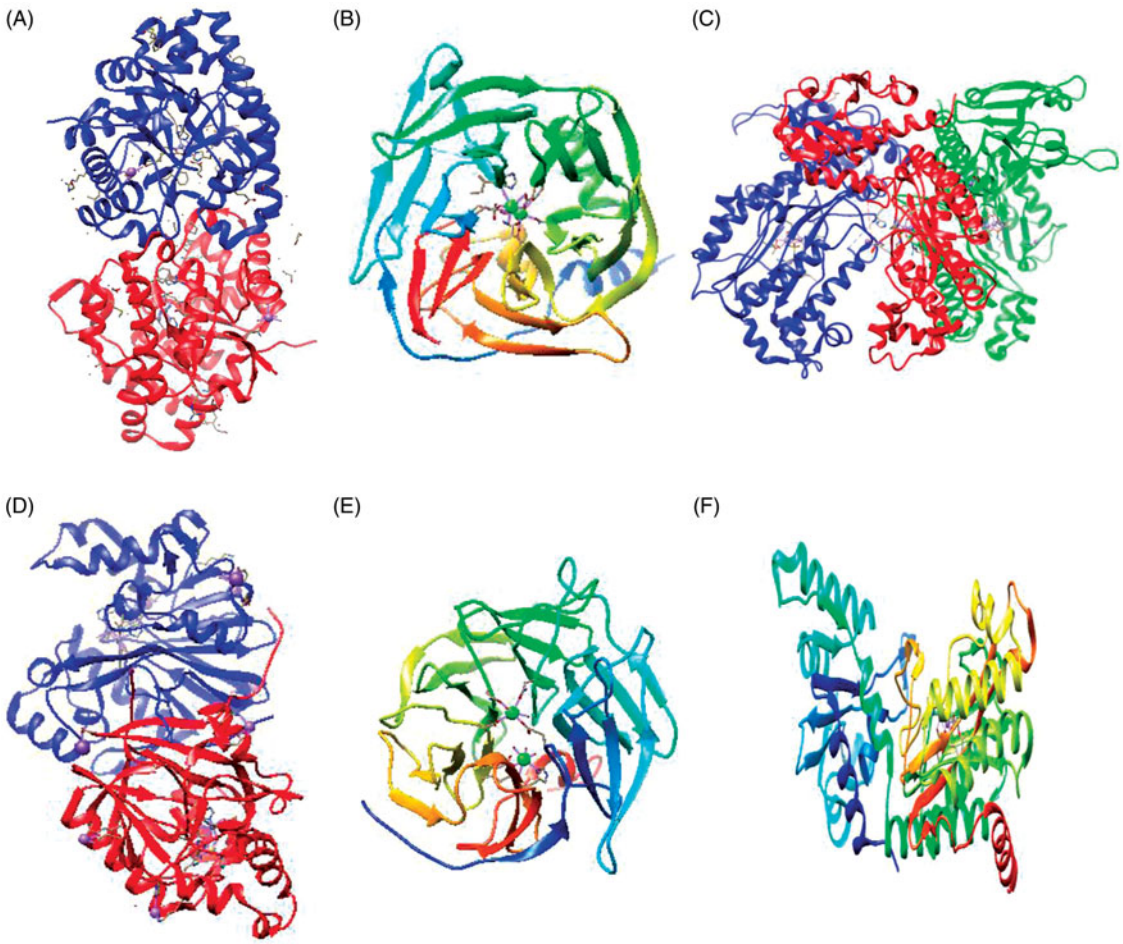

Figure 4. Structure of OP degrading enzymes. (A) PTE from *Pseudomonas diminuta* (OPH) "1HZY": Two chain metalloprotein with 46 helices and 6 sheets and the Zinc as its central atom. It belongs to the alpha and beta protein class having a TIM beta/alpha barrel-fold (Benning et al. 2001) (B) Serum Paraoxonase "1V04": Single chain beta class metalloprotein with central calcium binding site, 4 helices, 5 sheets, and 6 bladed beta-propeller fold (Harel et al. 2004). (C) OPAA "3L7G": It is a three chain metalloprotein having 54 helices and 6 sheets with central atom Manganese in its structure. The protein is capable of performing biological processes like depshosphorylation, proteolysis and respond to the toxic substances (Vyas et al. 2010). (D) MPH "1P9E": It is two chain metalloprotein with 20 helices, 7 sheets, and Zinc central atom. It belongs to the class of alpha and beta proteins (Dong et al. 2005). (E) DFPase "1E1A": It is a single chain Calcium-dependent PTE with 1 helices and 4 sheets in its structure, that belongs to the class of beta protein having 6-bladed beta-propeller (Scharff, Koepke et al. 2001). (F) Aminopeptidase P "1WL9" from *E. coli*, a protease with manganese at its center comprising of two domains. The C-terminal domain with the characteristic "pita-bread" fold is versatile, with the ability to execute a variety of catalytic functions. It belongs to the class of alpha and beta proteins and is capable of performing molecular functions such as peptidase activity, hydrolase activity and biological function like proteolysis (Graham et al. 2005).

Reaction mechanism

The enzymatic reaction mechanism of hydrolysis for organophosphate triesters involves binding of substrate to the binuclear metal ion at the active site of the enzyme. The binding occurs *via* the coordination of phosphoryl oxygen to one of the metal ions that weaken the hydroxide bridging between the metal ions. The distance between the metal and phosphoryl oxygen of the substrate is 2.5 Å. The bond between the metal and the oxygen polarizes the P—O bond and gives more electrophilicity to the phosphorus center. The hydroxide ion acts as a nucleophile and attacks the phosphorus center resulting in the weakening of the bond to the leaving group (Raushel 2002; Ghanem and Raushel 2005; Nath et al. 2016). The nucleophilic attack of hydroxide ion at the phosphorus center with the release of the leaving group is believed to be assisted by H254 by transferring a proton from D301 to the solvent and away from the active site. With the release of proton in the solvent the pH of the solvent decreases, this can be exploited for the detection of OPs. The formation of phosphorylated intermediate does not take place during the reaction mechanism because it proceeds by an SN2 mechanism which involves the inversion of stereochemistry at the phosphorus center (Ghanem and Raushel 2005). The rupturing of phosphorus oxygen bond is the rate-limiting step of the hydrolytic mechanism. Substrates with leaving group that possess a pKa value under seven are all hydrolyzed at the same rate, while substrates with the leaving group, that have pKa over seven, are hydrolyzed slower as pKa increases (Vilanova and Sogorb 1999).

The central metal ion plays three major roles in the hydrolysis reaction of organophosphate. The metal ion reduces the negative charge development on the leaving group by the process of neutralization. The metal ion increases the polarization of the P—O bond and thus enhances the electrophilicity at the phosphorus center, thereby it accelerates the attack of the hydroxyl ion. The metal ion may also increase the nucleophilicity of the attacking hydroxide ion and decrease the pKa of the bound water molecule (Raushel and Holden 2000).

Substrate specificity of OPH

OPH has quite a broad substrate specificity implying a plastic active site (Reeves et al. 2008; Wales and Reeves 2012). The broad substrate specificity is due to the nonspecific substrate binding site (Bigley and Raushel 2013). The rate-limiting step and the catalytic efficiency are dependent on the pKa of the leaving group (Ghanem and Raushel 2005). The enzyme is found to have the highest efficiency for hydrolyzing the electron withdrawing phenolic leaving groups, but it also cleaves the halide bond and thiol linkage (Bigley and Raushel 2013). The surface of the enzyme has three hydrophobic pockets, to which the three esters groups of substrates interact. The leaving group pocket is made up of the residues W131, F132, F306, and Y309. These residues largely govern the specificity of the leaving group. The other ester groups interact with the large and small pocket. This determines the specificity of the side ester groups of the substrate. In the hydrolysis reaction of organophosphate, the enzyme exhibits a significant amount of stereoselectivity. In the hydrolysis reaction of the racemic mixture, the enzyme prefers the S_p enantiomer over the R_p enantiomer. When the actual bond cleavage is the rate-limiting step, the corresponding phosphate esters are found to be hydrolyzed slower than the thiophosphate esters. And when the rate limiting step is associated with the conformational step or product release then the hydrolysis of phosphate esters is found to be faster than the thiophosphate esters (Raushel and Holden 2000; Bigley and Raushel 2013).

Enzyme activity of OPH

The enzymatic activity of OPH is influenced by temperature, pH, and substrate concentration. The activity of the enzyme varies with varying temperature. Initially, with the rise in temperature, the reaction rate also increases because of the increasing kinetic energy of the reacting molecule. Eventually, the kinetic energy of the reacting molecules crosses the threshold energy required for the breaking of hydrophobic and hydrogen bond that maintain the secondary structure. At this temperature, the structure of the active site changes resulting in the loss of catalytic activity because of denaturation of the enzyme. Therefore, OPH enzyme shows its maximum activity at an optimal temperature of 35 °C and pH of 7.5. Enzyme activity increases with increasing substrate concentration but once all the active site of the enzyme is occupied by the substrate no further increase in the activity of the enzyme is observed (Maheshwari et al. 2017).

Other organophosphorus hydrolyzing enzymes

There are a number of methods known for the degradation of OPs like incineration and chemical neutralization but, among all the advanced technologies known microbial enzyme mode of degradation is the safest. Although several OPs degrading enzymes have been identified in numbers of organisms including mammals, however, the microbial enzymes have sought more attention and have been found to be more potent in degrading OPs (Siddavattam 2017). OPs degrading enzymes were first time reported in 1946 by Mazur. These enzymes were later categorized in the category of phosphotriester hydrolase by the Nomenclature Committee of the International Union of Biochemistry and Molecular Biology. These enzymes were further classified based on their substrate specificity (Raushel 2002). Although OPH is the most studied and well-categorized among all OP degrading enzymes, other enzymes have also been reported which are capable of detoxifying OPs (Theriot and Grunden 2011). Table 1 shows the comparison of known organophosphorus degrading enzymes.

Paraoxonase (PON)

PON enzyme in human serum has the ability to degrade paraoxons and nerve agents. Its structure revealed that it is a Ca containing monomer enzyme (Figure 4(B)). It is a single chain beta class metalloprotein with central Calcium binding site, 4 helices, 5 sheets and 6 bladed beta-propeller (Harel et al. 2004). Human paraoxonase preferably cleave bonds like P—O, P—C, P—F, and P—CN (Di Sioudi et al. 1999). A variant of mammalian paraoxonase is found to be more efficient for the degradation of some OPs like cyclosarin and soman than OPH and DFPase (Amitai et al. 2006).

Organophosphorus acid anhydrolase (OPAA)

Organophosphorus acid anhydrolase (OPAA) is an enzyme isolated from the extract of halophilic *Alteromonas* species and is found to be able to hydrolyze a large number of OPs. Figure 4(C) shows the crystal structure of OPAA (Jacquet et al. 2016). It is a monomeric 58 kDa polypeptide metalloprotein having Mn in its natural form. It is able to hydrolyze organophosphate triesters and the protein appears to be dipeptidase (Raushel 2002; Vyas et al. 2010). It displays stereo specificity similar to PTE, but the rate of hydrolysis is slightly less than that of PTE. It also shows high activity in hydrolyzing the P-F bond in OPs like sarin, soman, and DFP. However, it is less effective in hydrolyzing P—CN, P—O bond and is unable to hydrolyze P—S bonds (Raushel 2002).

Methyl parathion hydrolase (MPH)

MPH belongs to a family of metallo beta lactamase and is an aryldialkyl phosphatase (Figure 4(D)). The first *mpd* encoding gene for MPH was identified in *Plesiomonas sp.* strain M6 (Jacquet et al. 2016). Another closely related gene was identified and sequenced from *Pseudomonas sp*. WBC3. Its structure revealed that it is a Zn containing homodimer enzyme. It catalyzes the degradation of methyl parathion. Each subunit consists of hybrid binuclear Zn in which most solvent exposed β metal cation is replaced with Cd. It is found to be homologous to other metal β lactamases but does not show any similarity to PTE (Jacquet et al. 2016).

Table 1. Features of OP compound degrading enzymes.

Enzyme	Isolated from microorganism	Bonds cleaved by the enzyme					Metal ion	Active form of enzyme	Size	Substrate specificity	Reference
		P—O	P—F	P—CN	P—S	P—C					
Organophosphorus hydrolase (OPH)	*Pseudomonas diminuta, Flavobacterium, Agrobacterium radiobacter*	✓	✓	✓	✓	×	Zn	Dimer	36 kDa	Paraoxon, DFP, VX, Soman, Mipafox, Dursban, Parathion, Coumaphos, Diazinon, Fensulfothion, Methylparathion, Cyanophos, Acephate, Azinophos-ethyl demethon-S, Malathion, Phosalone, Methamidophos, tetriso (Sp)-EPN	Di Sioudi et al. (1999); Vilanova and Sogorb (1999); Benning et al. (2001); Karpouzas and Singh (2006)
Paraoxonase (PON)	Human	✓	✓	✓	×	✓	Ca	Monomer	43 kDa	Alkyl fluorophosphate, Paraoxon, Soman, DDVP, Glyphosate	Di Sioudi et al. (1999)
Organophosphorus acid anhydrolase (OPAA)	*Alteromonas* sp. JD6.5, *Pseudoalteromonas haloplanktis*	✓	✓	✓	✓	×	Mn	Monomer	58 kDa	Paraoxon, DFP, Soman, Sarin, Mipafox	Di Sioudi et al. (1999; Vilanova and Sogorb (1999); Karpouzas and Singh (2006); Daczkowski et al. (2015)
Methyl parathion hydrolase (MPH)	*Pseudomonas* sp. WBC 3	✓	×	×	×	×	Zn	Dimer	34 kDa	Methyl parathion, Parathion, Paraoxon	Chu et al. (2003); Liu, Hong, et al. (2007); Farnoosh and Latifi (2014)
Di-isofluoro-phosphatase (DFPase)	*Loligo vulgaris*	×	✓	×	×	×	Ca	Monomer	35 kDa	DFP, Tabun	Di Sioudi et al. (1999)
Aminopeptidase P	*Escherichia coli*	Amino-terminal X-pro peptide bond					Mn	Tetramer	49.65 kDa	p-nitrophenyl methyl phosphonates, Paraoxon, Substrate consisting of methyl isopropyl and methyl isobutyl group	Yoshimoto et al. (1989); Jao et al. (2004); Graham et al. (2005); Farnoosh and Latifi (2014)

Diisopropyl-fluorophosphatase (DFPase)

DFPase is a 35 kDa monomer protein obtained from the brain of *Lolilgo vulgaris* squid (Figure 4(E)). DFP is the main substrate and hydrolyze P—F bond releasing isopropyl phosphate and fluoride. Two highly effective calcium sites are required for its stabilization and catalysis function. To identify the residues important for the active site and to decipher the reaction mechanism of the enzyme, site directed mutagenesis and kinetic studies were performed (Hartleib and Rüterjans 2001; Scharff, Koepke et al. 2001; Scharff, Lücke et al. 2001; Katsemi et al. 2005). Three histidine residues were found to play an important role at the active site, in which two histidine H274 and H174 have the role of stabilization and residue H287 was found to act as a general base catalyst (Jacquet et al. 2016).

Aminopeptidase P (pep P)

It is an exopeptidase of 49.65 kDa that cleaves the N-terminal residue from a polypeptide when the second residue is proline. It is a tetrameric metalloprotein in *Escherichia coli* that consists of four Pep monomers and requires two Mn ions for its activity (Farnoosh and Latifi 2014). The enzyme adopts "pita bread" fold like creatinase and methionine aminopeptidase that functions as a tetramer (Ghanem and Raushel 2005). The two manganese ions in the active site at the C terminal of the β sheet are separated by 33 Å. The two ions bridge together *via* a hydroxide ion which acts as the nucleophile in the attack of the peptide bond (Figure 4(F)) (Karpouzas and Singh 2006). Its substrate for degradation includes methyl isobutyl and methyl isopropyl groups (Farnoosh and Latifi 2014). Incidentally, it shows only 31% sequence similarity with OPAA (Theriot and Grunden 2011).

Among the OP compound degrading enzymes, OPH demonstrates wider substrate activity that includes P—O, P—F, P—CN, and P—S bonds (Table 1). OPH shows its activity on substrates such as paraoxon, DFP, VX, soman, mipafox, dursban, parathion, coumaphos, diazinon, fensulfothion, methyl parathion, cyanophos, acephate, azinophos-ethyl demethon-S, malathion, phosalone, methamidophos, tetriso, and (Sp)-EPN, making it a favorable candidate for biosensor and bioremediation studies. Similar to OPH, OPAA also shows wider substrate specificity, and thus can be used for detection as well as for bioremediation applications. Interestingly, human Paraoxonase is the only reported enzyme which can cleave P—C bond compounds, and reported to be more efficient for the degradation of some OPs like cyclosarin and soman than OPH and DFPase (Amitai et al. 2006).

Mechanisms of biosensing detectors

Typically, the detection systems used in conjunction with biological components can be classified into electrochemical (potentiometric, amperometric, and conductometric) and optical (UV–visible and fluorescence) systems of measurement. Detection systems employing potentiometric measurement utilize changes in potential with corresponding changes in current which is the result of oxidation and reduction potential of the electrochemical reaction. On the other hand, amperometric detection systems work on the basis of changes in current according to changes in chemical concentrations of interest. They typically utilize two/three electrodes systems constituted as a reference, a working electrode and an auxiliary electrode. Amperometric detection systems are believed to be superior due to the linear increase which solves the perils, such as salt screening and exponential or logarithmic increase with the concentration in a potentiometric detection system. The conductometric detection systems measure electrical conductivity or resistivity of analyte samples based on the number of ions and electrons. The effect produced is also influenced by temperature and pH. Electrical impedance is another phenomenon utilized by detection systems wherein the resistance of biological component and ionic conductance across it is utilized for the measurement. The optical detection systems typically utilize photons as mediating components in electrical transduction in comparison to direct use of electrons in electrochemical detectors. Intensity, decaying time, quenching efficiency, radiant energy transfer, anisotropy, etc. are the critical parameters measured while using absorption, reflectance or fluorescence using ultraviolet (UV), visible, near-infrared (NIR) radiations in photometric measurement. Some optical detection tools also work on the principle of evanescent waves and total internal reflection phenomenon occurring due to the changes in the refractive index. Some hybrid mechanisms like electrochemiluminescence, amperometric-potentiometric, piezoelectric, and magneto-elastic detection systems are also utilized in several reports of biosensors.

Biosensors for detection of OPs using OPH

The currently accepted and utilized methods for detection and quantification of OPs such as liquid chromatography or immunoassay-based techniques have limitations of being time-consuming, non-suitable for infield determination and online monitoring. Lately, biosensors have emerged as leading analytical techniques owing to miniaturization of transduction, development of microelectronic circuitry and interfacing using bio-recognition units. Cost effective and miniaturized analytical tools have led to the transformation of sophisticated instruments into the point-of-care devices. Enzymes are the most commonly utilized biological recognition units considering the ease of application and translation. Analysis of OPs can best be investigated using OPH as a biological recognition unit and converting the catalytic reaction to a measurable signal in a biosensor. The broad substrate specificity of OPH makes it an attractive enzyme of interest for researchers and professionals interested in monitoring and detoxification of OPs present in the environment. The OPH catalyzed hydrolysis reaction of OPs generates two protons and an alcohol, which can be chromophoric or electroactive. This provides ample opportunities for use of OPH in a variety of sensors ranging from fluorometric to electrochemical, or even a pH-based sensor that can quantify changes in pH based on the increase in protons generated during the hydrolysis process. A broad classification of the various

biosensors employing OPH for detection of OPs is described here.

Electrochemical

A typical electrochemical sensor (Table 2) is based on the processes occurring inside an electrochemical cell, in which the working electrode (usually glassy carbon electrode or a conductive strip) is coated with the compound of interest, while the analyte (or substrate) is inserted into the electrolyte of the electrochemical cell. Here, sensing is based on changes in current and/or voltages upon addition of analyte to the electrolyte. Additionally, a transducer, amplifier, and a data analysis system are other components included which define the biosensing performance of electrochemical biosensors. Property of electrodes is the key determining factor in the performance using this electrochemical catalysis. The basis of detection can be the changes in current or potential differences occurring at the biological receptor–electrode interface. In the case of OPH, OPs (such as methyl parathion or paraoxon) are the analytes introduced in specific concentrations into the electrolyte (Figure 5). The basis of detection, various approaches and materials employed, using electrochemical methods have been described in the following sections.

Amperometric

Amperometric sensors record changes in the electric current at a fixed potential for a given electrolyte, working electrode, and analyte concentrations. The relatively low-cost setup and potential for high sensitivity have made amperometry a popular technique for developing biosensors. Immobilization of OPH on the electrode surface is the most common method to deploy the amperometric enzyme-based assay. The advent of nanoscience and materials engineering approaches have further led to novel modifications of electrode surfaces with nanomaterials and complex material architectures. This has resulted in enhanced biosensor performance owing to the efficient stabilization of biomolecules and charge transfer mechanisms. Several nanomaterials such as carbon nanotubes, zinc oxide nanoparticles with multiwalled carbon nanotubes (MWCNT), gold nanoparticles, gold–platinum bimetallic nanoparticles, silver nanoparticles, nanocomposites of MWCNT-Au with a glassy carbon electrode, zirconium dioxide/chitosan with glassy carbon electrodes have been investigated for developing improved amperometric biosensors. Du et al. developed a nanomaterial-based biosensor by covalent coupling of OPH loaded quantum dots with carbon nanotubes/gold composites with a detection limit of 1.0 ng/mL (Du et al. 2010). Trojanowicz et al. immobilized OPH on MWCNT modified graphite working electrode and performed amperometric experiments with paraoxon in the presence of Co in solution. They obtained a sensitivity of 12.8 nA/μM, with a linear range of 0.5–30 μM and a detection limit of 0.52 μM for paraoxon (Trojanowicz et al. 2004). Apart from the nanomaterials, mesoporous materials have been utilized very commonly to modify glassy carbon electrode. An example of such a modification of glassy carbon electrode using mesoporous carbon/carbon black was described by Lee et al., who showed that OPH immobilized electrode showed a high sensitivity of 198 nA/μM with a linear range of 0.2–8 μM and a detection limit of 0.12 μM for paraoxon. The use of mesoporous carbon/carbon black electrode provided an improvement of sensor performance in comparison to a carbon nanotube-based modification of glassy carbon electrode which gave a linear range of 0.25–4 μM and a detection limit of 0.15 μM (Table 2.1). The detection is based on the anodic oxidation of *p*-nitrophenol, which is a degradation byproduct of OPs (Deo et al. 2005; Lee et al. 2010). Another application of mesoporous materials was employed using OPH immobilized silica modified glassy carbon electrode crosslinked with glutaric dialdehyde (GDAH). This approach showed a detection limit of 0.4 μM, with over 96% recovery of paraoxon when tested in simulated real samples, including soapy water, biomass, clay colloids, and river water (Lei, Valenta et al. 2007). Miniaturization of the electrodes in the form of screen-printed carbon electrodes has also transformed the biosensors closer to the point-of-care amperometric biosensor devices. Screen printed carbon electrodes using OPH in a Nafion binder described by Mulchandani et al. showed a detection limit of 0.07 μM for methyl parathion and 0.09 μM for paraoxon, respectively, with a sensitivity of 2.83 and 1.67 nA/μM, respectively, for methyl parathion and paraoxon (Table 2.1) (Mulchandani, Mulchandani, Chen et al. 1999).

Alternatively, the whole cells expressing OPH can also be used for measurement of OPs. Whole cells of *E. coli*, *Pseudomonas putida*, *Moraxella* species expressing OPH either intracellularly or on the surface of cells have been immobilized on the electrode surface. One such biosensor employing whole cells of *Moraxella sp.* was developed by Mulchandani et al. to show a limit of detection of 0.2 μM for paraoxon and 1 μM for methyl parathion, respectively (Table 2.1) (Mulchandani, Chen, Mulchandani, Wang, Chen 2001). Similarly, Tang et al. developed a mutant OPH using ice nucleation protein (INP) expressed on the surface of *E. coli* cells (BL21). The OPH-expressing bacteria aliquot was then added to a glassy carbon electrode already modified with ordered mesoporous carbon and Nafion. The sensor thus developed displayed limits of detection of 9.0, 10.0, and 15.0 nM for paraoxon, parathion, and methyl parathion, respectively, while the linear ranges for these compounds were 0.05–25 μM for paraoxon/parathion, and 0.08–30 μM for methyl parathion. The sensitivity obtained was 0.13 μA/μM with a stability of one month and 70% activity retention for paraoxon (Table 2.1) (Tang, Zhang et al. 2014). Lei et al. immobilized *P. putida JS444* cells expressing OPH on a carbon paste electrode, thus developing a working electrode for use as an amperometric biosensor for OPs. The sensor was able to oxidize *p*-nitrophenol at 0.6 V *vs.* Ag/AgCl and displayed low limits of detection of 0.28, 0.26, and 0.29 ppb, respectively, for paraoxon, methyl parathion and parathion (Lei, Mulchandani, Wang et al. 2005; Tang, Zhang et al. 2014). Likewise, Mulchandani et al. have reported modifying carbon paste electrodes with genetically engineered *Moraxella sp.* strain, which gives a detection limit of 0.2 and 1 μM, respectively, for paraoxon and methyl parathion (Mulchandani, Chen, Mulchandani, Wang, Chen 2001). Certain reports

Table 2. Characteristics of electrochemical based biosensors.

Cell type	Type (Material)	Substrate (LOD)	Linear range	Sensitivity	Stability	Response time	Reference
2.1 Amperometric biosensors							
E. coli	1. Nafion–OMCs, three-electrode system using bare GCE as working electrode and platinum wire as auxiliary electrode and saturated calomel electrode (SCE) as reference electrode	Paraoxon (0.009 μM) Parathion (0.010 μM) Methyl parathion (0.015 μM)	0.05–25 μM 0.05–25 μM 0.08–30 μM	0.13 μA/μM – –	70% activity for 1 month	–	Tang, Zhang et al. (2014)
	2. Single walled carbon nanotube (SWNTs) and, multiple carbon nanotube (MWNTs)	Paraoxon 0.01 μM for SWNT 6.4 μM for MWNT	0.5–8.5 μM 0.5–6 μM	0.0001 + 2.4 μA/μM (SWNT) 0.0002 + 0.17 μA/mM (MWNT)	25% activity loss over 7 months	–	Pedrosa et al. (2010)
	3. Carbon paste + Nylon net + silicon oil	Parathion (0.015 μM) Paraoxon (0.02 μM)	0.02– 0.18 μM –	21 ± 0.1 nA/μM 12 ± 0.8 nA/μM	>2 months	–	Lee et al. (2010) Chough et al. (2002)
	4. Thick Film electrode, OPH deposited on the electrode in Nafion film	Methyl parathion (0.07 μM) Paraoxon (0.09 μM)	0–9 M 0–25 μM	2.83 nA/μM 1.67 nA/μM	–	<10 s	Mulchandani, Mulchandani, Chen et al. (1999)
	5. OPH immobilized on cystamine coated gold thin film on insulated p-type silicon substrate in 3 electrode electrochemical cell.	Paraoxon (0.1 μM) Methyl parathion (0.1 μM)	1–10 μM	2.29 nA/μM 1.04 nA/μM	4 weeks	<40 s	Wang et al. (2003); Lee et al. (2010)
	6. Mesoporous carbon and carbon black modified electrode	Paraoxon (0.12 μM)	0.2–8 μM	198 nA/μM	–	<10 s	Lee et al. (2010)
	7. CNT-modified electrode with amperometric flow injection	Paraoxon (0.15 μM) Methyl parathion (0.8 μM)	0.25–4 μM Up to 2 μM	25 nA/μM 6 nA/μM	–	<10 s	Deo et al. (2005); Lee et al. (2010)
	8. OPH-modified carbon-paste working electrode, a Ag/AgCl reference electrode and a platinum wire counter electrode	Methyl parathion (0.4 μM) Paraoxon (0.9 μM)	0–5 μM 4.6–46 μM	2.14 nA/μM 1.45 nA/μM	160 min 280 min	Less than 6 s	Wang et al. (1999)
	9. Graphite electrode modified with MWCNT	Paraoxon (0.52 μM)	0.5–30 μM	12.8 nA/μM	–	2–3 min	Trojanowicz et al. (2004)
	10. Glassy carbon electrode, Horse radish peroxidase (HRP)	Dichlofenthion (24 μM)	25–500 μM	0.095 ± 0.024 nA/μM	–	10 min	Sahin et al. (2011)
E. coli pJK 33 + *Arthrobacter* sp.	Carbon paste electrode and cells casted in Nafion by drop casting	Paraoxon (10 nM) Methyl parathion (20 nM)	0–5 μM	3.979 nA/μM 0.989 nA/μM	2 d at 4 °C	<5 min	Lei et al. (2004)
Moraxella sp.	1. 3-electrode electrochemical cell, with whole cell modified carbon paste electrode, Faraday cage, Ag/AgCl electrode, Platinum wire auxiliary electrode	Paraoxon (0.2 μM) Methyl parathion (1 μM)	Up to 40 μM Up to 175 μM	12.24 ± 0.39 nA/ μM 1.49 ± 0.02 nA/μM	45 d at 4 °C	2 min	Mulchandani, Chen, Mulchandani, Wang, Chen et al. (2001)
P. putida JS444	1. Carbon paste electrode, electrochemical cell setup	Paraoxon (0.001 μM) Methyl parathion (0.001 μM) Parathion (0.001 μM) Thiobenzenephosphonate (0.00494 μM) Fenitrothion 0.00505 μM)	Up to 2 μM Up to 5 μM 	20.50 nA/μM 17.57 nA/μM 19.13 nA/μM 8.22 nA/μM 10.35 nA/μM	5 d at 4 °C 5 d at 4 °C 	Less than 5 min Less than 5 min 	Lei, Mulchandani, Wang et al. (2005) Lei, Mulchandani et al. (2007)

(*continued*)

Table 2. Continued.

Cell type	Type (Material)	Substrate (LOD)	Linear range	Sensitivity	Stability	Response time	Reference
2.2 Potentiometric biosensors							
E. coli	1. OPH expressed on cell surface, hydrogen ion sensing glass membrane of the pH electrode	Paraoxon (2 μM) Methyl parathion (2 μM) Diazinon (5 μM)	0.055–1.8 mM 0.06–0.91 mM 0.46–8.56 M	90.62 mV/decade 53.24 mV/decade 45.1 mV/decade	Over 2 months at 4 °C	Steady mode: 10 min. Kinetic mode: 2 min	Mulchandani, Mulchandani, Kaneva, Chen (1998)
	2. Hydrogen ion sensing membrane of pH electrode, Bovine serum albumin and glutaraldehyde	Paraoxon (2 μM) Parathion (2 μM) Methyl parathion (2 μM) Diazinon (5 μM)	0.15–0.7 mM 0.06–0.47 mM 0.1–0.43 mM 0.13–2.8 mM	150.44 mV/decade 64.96 mV/decade 68.99 mV/decade 53.18 mV/decade	1 month	10 min. (steady state), 2 min. (kinetic)	Mulchandani, Mulchandani, Kaneva, Chen (1999)
	3. Microbial-based potentiometric electrode	Paraoxon (3 μM)	–	–	58% activity retained after 24 h	Steady mode: 10 min.; Kinetic mode: 2 min.	Mulchandani, Mulchandani, Chauhan et al. (1998)
	4. Flow cell containing biomass transducer and pH glass electrode	Paraoxon (1.8 μM)	0.001–1.0 mM	–	Over 2 months at 4 °C	Batch reactor: 10 min.; Flow through system: 20 min	Rainina et al. (1996)
	5. H + selective electrode	Paraoxon (5 μM) Diazinon (5 μM) Parathion (5 μM) Chlorpyrifos (5 μM)	0.05–0.4 mM 0.05–0.35 mM 0.007–0.05 mM 0.01–0.15 mM	98 mV/decade 61 mV/decade 37.7 mV/decade 24.6 mV/decade	60% activity up to 70 d	5 min	Gäberlein et al. (2000)
	6. Wearable Tattoo sensor: OPH/Nafion/PVA hydrogel drop casted on electropolymerized polyaniline (PANI) coated screen printed electrodes	Di-isopropyl fluorophosphates (10 mM)	10–120 mM	–	5 d	<20 s	Mishra et al. (2018)
2.3 Conductance based electrochemical biosensor							
P. diminuta	1. OPH immobilized on beaker surface; carbon nanotube paste electrode as working electrode in 3 electrode cell with OPH-immobilized beaker surface	Methyl Parathion (0.1 μM)	0.1–200 μM	–	50% activity over 50 d at 4 °C	≥10 min	Gothwal et al. (2014)
P. putida JS444	1. OPH immobilized on SWCNT electrode	Paraoxon (50 μM)	50–250 μM	–	–	–	Liu, Cai, et al. (2007)
2.4 Dissolved oxygen based electrochemical biosensors							
Moraxella sp.	1. Polycarbonate membrane coated with cell suspension and buffer on top of dissolved oxygen electrode	Paraoxon (0.1 μM)	0.05 mM	0.61 Δ% O_2 consumed/μM	1 week	<5 min	Mulchandani et al. (2006)
P. putida JS444	1. Nucleopore polycarbonate membrane, oxygen electrode with Teflon membrane	Fenitrothion (277 ppb) EPN (1.6 ppm)	Up to 0.05 mM	0.10 % 0.20 %	5 d at 4 °C	<5 min	Lei et al. (2006)
		Methyl parathion (53 ppb) Paraoxon (55 ppb) Parathion (58 ppb)	0.2–50 μM 0.2–50 μM 0.2–50 μM	0.31 (Δ% O_2/μM) 0.31 (Δ% O_2/μM) 0.31 (Δ% O_2/μM)	5 d at 4 °C	>5 min	Lei, Mulchandani, Chen, et al. (2005)

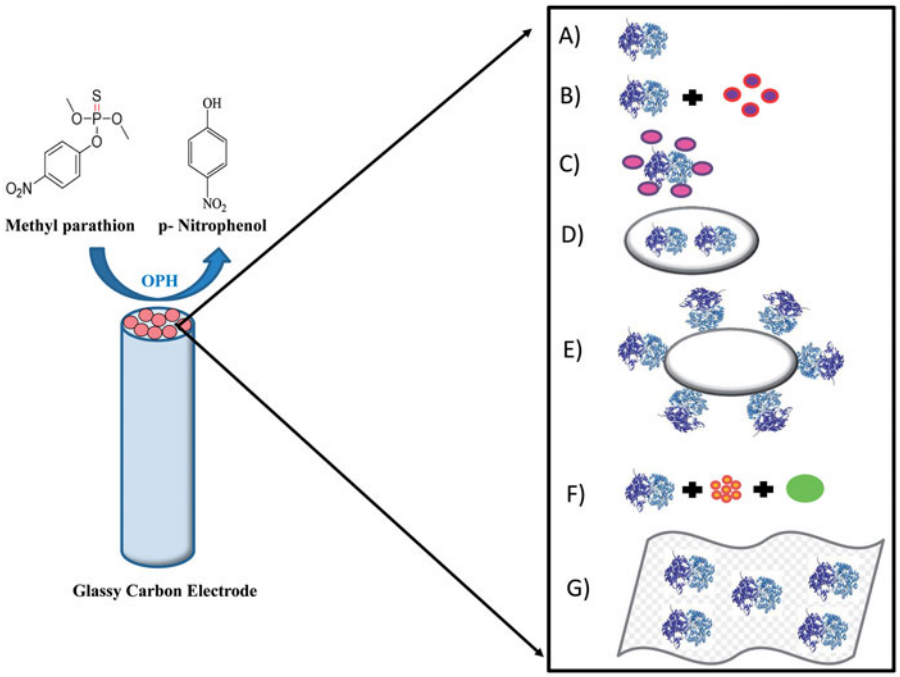

Figure 5. Schematic diagram of electrochemical sensing system: Glassy carbon electrode surface showing conversion of OP compound into *p*-nitrophenol (PNP), in the presence of OPH and the various configurations for developing electrochemical biosensor found in contemporary literature. (A) Only organophosphorus hydrolase. (B) Organophosphorus hydrolase with nanoparticle. (C) Organophosphorus hydrolase with quantum dots. (D) Organophosphorus hydrolase inside bacterial cell (E) Organophosphorus hydrolase on bacterial cell surface. (F) Organophosphorus hydrolase with gold nanoparticle and binder. (G) Encapsulated Organophosphorus hydrolase.

employ hybrid biorecognition units like enzyme-microorganisms or enzymes-tissues etc. for the detection of analytes. On this principle, a hybrid system containing OPH enzyme and *Arthrobacter* sp. JS443 were co-immobilized in a carbon paste electrode by Lei et al. This combination is meant for the formation of *p*-nitrophenol by OPH and subsequent utilization of *p*-nitrophenol by enzymatic systems present in the *Arthrobacter* sp. About 10 nM of paraoxon and 20 nM of methyl parathion were detected using such a biosensor with a good repeatability (40 times) and a storage shelf-life of 2 d. A poor shelf life has been described due to a reduced nutrition and consumption of NADPH over a period of time by the cells (Lei et al. 2004).

Among the literature reports for amperometric biosensing, greater detection limits are obtained by Lei et al. with 0.001 μM (paraoxon, methyl parathion, and parathion) when they used a carbon paste based electrode to immobilize *P. putida* (Lei, Mulchandani, Wang et al. 2005). However, the stability of this biosensor was reported to be only 5 d when stored at 4 °C. The best stability with only 25% activity loss over 7 months was observed in the sensor developed by Pedrosa et al. when they interfaced OPH with carbon nanotubes (Pedrosa et al. 2010). A broad linear range (0.05–25 μM for paraoxon and parathion) was reported by Tang et al. in a biosensor developed by modifying glassy carbon electrode surface with ordered mesoporous carbon and immobilizing engineered *E. coli* strain expressing OPH at the cell surface using Nafion (Tang, Zhang et al. 2014). In the higher concentration segment, an improved linear range of 25–500 μM (for dichlofenthion) was observed in a co-enzyme modified (OPH + HRP) glassy carbon electrode sensor developed by Sahin et al. (2011). Interestingly, a higher sensitivity (198 nA/μM) and lower response time (<10 s) were observed by Lee et al. using a mesoporous carbon/carbon black based sensor immobilized with OPH (Lee et al. 2010). Though amperometric sensors are known for their good sensitivity and low detection limit, they are susceptible to noise and the results are often affected by instantaneous phenomena at the electrode–electrolyte interface. In cases where there may be complex interactions between analytes and/or solutions, potentiometric methods may be more preferable (Zhang 2004).

Potentiometric

In potentiometric methods of sensing, voltage is measured between two electrodes in a no-current situation. The measured potential is then used to determine the concentration of a particular component. However, for the purpose of observing the action of OPH on OP compounds, the liberation of H^+ ions by the hydrolytic reaction of OPH with OPs is determined by pH-sensitive electrodes or transducing materials. The result is displayed as a series of displacements after addition of OPs on an otherwise constant graph of voltage *vs.* time. Potentiometric biosensors developed for detection of OPs predominantly are formed from immobilized cells expressing OPH. Pure OPH enzyme based biosensors which use potentiometric detection are meager. One of the reports of such isolated enzyme (OPH) based biosensors by Mulchandani et al. consist of a hydrogen ion sensitive pH electrode modified by OPH using glutaraldehyde as a linker. The limit of detection was reported to be 2 μM for paraoxon, parathion, and methyl parathion and 5 μM for diazinon, with a best-case linear range of paraoxon, 0.15–0.7 mM in a 1 mM

HEPES buffer (Table 2.2) (Mulchandani, Mulchandani, Kaneva, Chen 1999). Gaberlein et al. developed a disposable potentiometric biosensor by immobilizing OPH on an ion selective electrode developed using double membrane matrix (filter paper and PVC) technology. This biosensor was able to reach a detection limit of 5 μM for paraoxon, diazinon, parathion, and chlorpyrifos with a linear range of 0.05–0.4, 0.05–0.35, 0.007–0.05, and 0.01–0.15 mM, respectively (Gäberlein et al. 2000). In order to reduce the effects of passivation produced in a potentiometric pH sensitive field effect transducer a layered structure formed from Ta_2O_5 on SiO_2 and p-Si was developed by Schoning et al. as an Electrolyte-Insulator-Semiconductor (EIS) type capacitance based biosensor to investigate effects of adsorption, crosslinking and entrapment of OPH on the electrode surface. They described a detection limit of 2 μM and a linear range of 10–100 μM (Schöning et al. 2003). This method also provided a photolithography-less miniaturized capacitance based measurement system.

Use of whole cells expressing OPH either intracellularly or on the surface is very common for developing potentiometric biosensors. Mulchandani et al. reported an impressive linear range of 0.46–8.56 mM for diazinon in a pH electrode sensor modified with *E. coli* cells expressing OPH on the cell surface (Table 2.2) (Mulchandani, Mulchandani, Kaneva, Chen 1998). Furthermore, Mulchandani et al. observed the best sensitivity for paraoxon 150.44 mV/decade concentration in a sensor based on the deposition of OPH on top of the glass membrane in a pH electrode (Table 2.2) (Mulchandani, Mulchandani, Kaneva, Chen 1999). In another study by the same group of researchers, direct immobilization of cell suspensions expressing OPH at the surface on the exposed surface area of a pH sensitive hydrogen ion sensor produced the detection limit of 2 μM for paraoxon, methyl parathion, and 5 μM for diazinon. Furthermore, linear ranges for these three OPs was reported to be 0.055–1, 0.06–0.91, and 0.46–8.56 mM, respectively (Table 2.2) (Mulchandani, Mulchandani, Kaneva, Chen 1998). Rainina et al. developed a biosensor based on cryo-immobilization of *E. coli* cells expressing OPH by entrapment into the polyvinyl alcohol (PVA) gel. These cells were either suspended in a batch reactor with pH electrode or packed in a column and placed upstream of a flow cell with a pH electrode. This yielded a low detection limit 1.8 μM and linear range 0.001–1 mM with the stability of over 2 months and low response time of 10 min (batch reactor) for paraoxon (Table 2.2) (Rainina et al. 1996). A novel wearable sensor for detection of DFP was developed so that sufficient warning can be provided in case of personal exposure to nerve agents so that measures to counter the poisoning can be taken. The research comprised of a printed tattoo sensor by electropolymerization of PANI and drop casting both Nafion/OPH enzyme in a PVA-based hydrogel layer on a screen-printed electrode. DFP estimation in liquid and vapor phase was possible by adsorption in hydrogel and contact with OPH can lead to the formation of the HF and P—OH group. This has led up to 10 mM detection within 20 s and a linear range of 10–120 mM (Mishra et al. 2018). The same group have utilized OPH in certain wearable platforms like rings, gloves, microneedles, or textiles for detection of OP compounds like methyl paraoxon, methyl parathion focusing toward detection of nerve agents in security applications (Mishra, Hubble et al. 2017; Mishra, Vinu Mohan et al. 2017; Sempionatto et al. 2017). Most of the reports of potentiometric biosensors have been described using OPH isolated from *E. coli* or cells expressing OPH. Highly sensitive detection (150.44 mV/decade concentrations) of paraoxon was obtained by a hydrogen ion sensing pH electrode employing crosslinked BSA with 1 month stability and a smaller linear range. Cell immobilized biosensors have been investigated to a greater extent using potentiometric methods and have provided with a storage stability of over 2 months along with a pH electrode (Mulchandani, Mulchandani, Kaneva, Chen 1998). Owing to the use of cell-based biosensors the response time of reported potentiometric biosensors has been in the range of 5–10 min. The lowest limit of detection (1.8 μM) was shown by Rainina et al. using a flow cell-based biosensor with a pH electrode (Rainina et al. 1996) with an enhanced linear range and stability. Other species of organisms like *P. putida* or *Moraxella* species have not been investigated to a great extent using potentiometric transducing methodologies which have found to be showing results with amperometric techniques (Mulchandani, Mulchandani, Kaneva, Chen 1998, 1999). Incidentally, potentiometric methods generally have found to have higher selectivity compared to amperometric methods due to the dependence on impedance rather than electrochemical cell parameters, as impedance characteristics tend to stay constant for a given material. However, the limit of detection may suffer, thus making other methods more preferable (Monroe 1989).

Dual amperometric–potentiometric

Simultaneous amperometric–potentiometric measurements of OPs can enhance the capabilities of biosensors by avoiding the false positives. The potentiometric estimation in such cases involves detection of protons produced in the catalytic reaction whereas amperometric estimation indicates the detection of *p*-nitrophenol. A report by Wang et al. have used such a dual amperometric–potentiometric detection of OPs using a flow injection assembly with an amperometric gold-silicon based electrode fabricated using photolithography tools and OPH immobilized on this electrode using cystamine and glutaraldehyde. The potentiometric transducer constituted of silicon based pH sensitive electrolyte (tantalum pentoxide)-insulator (silicon dioxide)-semiconductor (EIS) transducer was developed and run in a constant capacitance mode. Amperometrically, the detection limits were enhanced to about 70 nM for paraoxon with a linear range of 2–14 μM. Potentiometrically, detection limits of 2 μM paraoxon and 6 μM dichlorvos were estimated on the basis of the signal-to-noise characteristics for paraoxon and dichlorvos with an investigated linear range of 10–100 μM. Sensitivities of estimation obtained were 0.286 and 0.155 mV/μM with amperometric and potentiometric estimation, respectively. The study has been extended to four OP compounds (paraoxon, parathion, dichlorovos, and diazinon) in another report by the same group using a similar setup. The combined information obtained from both types of detection coupled with different biological recognition units can provide greater

information and minimize false (negative or positive) alarms (Wang et al. 2002; Schöning et al. 2003).

Conductometric

In this method, the change in current to a specific voltage input is recorded, either through a linear sweep over a voltage range or a pulse train superimposed on the linear sweep. Gothwal et al. deposited OPH extracted from *P. diminuta* bacteria on the inner surface of a polyvinyl chloride beaker, which was used as the reaction cell for a 3-electrode electrochemical setup in which a carbon nanotube-based carbon paste electrode was chosen as the working electrode. The working electrode was then used to catalyze the redox reactions of *p*-nitrophenol. The reported linear range for this sensor was found to be 0.1–200 μM with methyl parathion as a substrate, and for the same substrate, the response time and sensitivity were found to be 10 min and 0.003 μA/μM, respectively. The sensor retained 50% activity over 50 d (Gothwal et al. 2014). Kumar and D'Souza immobilized recombinant *E. coli* cells displaying a periplasmic expression of OPH on a screen printed glassy carbon electrode using glutaraldehyde. This sensor was then used to detect OPs *via* cyclic voltammetry based on the redox properties of *p*-nitrophenol and a limit of detection of 0.5 μM, the response time of 5 min and a linear range of 2–80 μM was observed with up to 80% retention of activity after 22 d for methyl parathion (Kumar and D'Souza 2011b; Gothwal et al. 2014). Kumar and D'Souza et al. have obtained impressive detection limits of 0.5 μM, a lower response time of 5 min and high stability i.e. 80% activity retained after 22 d for methyl parathion (Kumar and D'Souza 2011b). The widest linear range was observed in the sensor developed by Gothwal et al. 0.1–200 μM for methyl parathion (Gothwal et al. 2014). Liu et al. immobilized OPH on the single walled carbon nanotubes (SWNTs) based on the principle of dielectrophoresis, *via* bridging two (Ti/Au) electrodes patterned on the SiO_2 layer on the top of a Si substrate. They obtained a detection limit of 50 μM and a linear range of 50–250 μM using paraoxon, however, non-linearity was reported for concentrations below 50 μM (Liu, Cai, et al. 2007). Mulyasuryani et al. have immobilized OPH isolated from *P. putida* on chitosan which is coated over screen-printed electrodes. The enzyme was obtained by precipitation method using ammonium sulfate and was able to detect 40 ppb (diazinon), 30 ppb (malathion), 20 ppb (chlorpyrifos), and 40 ppm (profenofos) with up to 32 μS/ppb sensitivity (Mulyasuryani and Prasetyawan 2015).

In general, amperometric biosensors have the lowest limits of detection for OP compounds with a comparatively high stability, low response time, and good linear range, while potentiometric methods have better sensitivity. Comparative studies have suggested that voltammetric methods have a lower limit of detection compared to potentiometric methods at the cost of substrate specificity (Muratova et al. 2015).

Optical sensors

Most of the reports on optical sensors (Table 3) are based on the changes in absorbance or fluorescence during hydrolysis of OPs through the generation of byproducts like *p*-nitrophenol and the resultant change in the pH of the medium, which can be measured by the output of a UV–Vis spectrophotometer or a fluorescence spectrophotometer. Changes in absorbance due to the production of *p*-nitrophenol during the catalytic activity of OPH are the main mechanism of use of UV–Vis based detection of OP compounds. Quenching of fluorescence due to pH changes and employing pH-sensitive fluorophores forms the most common mechanism for the use of a fluorescence-based OPH biosensor (Figure 6).

UV–vis based sensors

UV–Vis based sensors refer to a type of optical sensing wherein a change in absorption upon creation of hydrolysis product of OPs is measured. In this case, however, the change is quantified either by means of measuring the signal from an optical fiber system, or directly using UV–visible spectrophotometers or plate readers. The principle of evanescent field optical fiber-based biosensors, in which an evanescent field is created by the presence of an extremely thin cladding on a dense core by means of total internal reflection at the interface, has also been used by several authors due to their convenience, lower cost and easy-to-deploy characteristics in various kinds of sensors. In terms of OPs detection and sensors, both enzymatic and cell-based detection methodologies have been investigated. Fiber optic detection mechanisms are very commonly described in literature while investigating OPH based UV–vis or fluorescence-based sensors owing to their portability, cost, and ease of use. In a report of enzyme immobilization by Mulchandani et al. who used an optical fiber based biosensor by immobilizing OPH on a nylon membrane attached to a sensor tip composed of a bundle of optical fibers. This system was attached to a measurement system comprising of a light source in which 400 nm light is delivered, a cutoff filter, reaction chamber, and an optical fiber system. The output measurement consists of a photomultiplier tube which can quantify changes in absorbance (at 400 nm) due to the generation of *p*-nitrophenol. Using this assembly of sensor tips a detection limit of 2 μM for paraoxon and parathion and 5 μM for coumaphos was reported (Table 3.1) (Mulchandani, Pan, Chen 1999). In another study, Zourob et al. described another way of using immobilized OPH in a pH sensitive matrix and estimating using a waveguide sensor developed from absorber material-clad, using solvent blue and polythiopene as clad layers and a sol–gel layer as a wave-guide. The principle of detection here was the change in refractive index when OPH enzyme was immobilized in a pH sensitive matrix containing OPs. This sensor was able to achieve a detection limit of 4 nM for paraoxon and parathion, with 81 nM for diazinon, with a linear range of 1–5 μM (Zourob, Ong et al. 2007).

A direct whole cell-based biosensor utilizing *Flavobacterium* sp. expressing OPH was developed by Kumar et al. who immobilized the cells on the glass fiber filter paper discs and analyzed methyl parathion. The absorbance of *p*-nitrophenol was measured in a specially designed reaction vessel connected through optical fibers to a UV–Vis

Table 3. Characteristics of OPH based optical-based biosensors.

Cell type	Type (material)	Substrate (LOD)	Linear range	Sensitivity	Stability	Response time	Reference
3.1 UV Spectrophotometric biosensors							
E. coli	1. Reversible inhibition of OPH by copper complexed meso-tri (4-sulfonatophenyl)mono(4-carboxyphenyl)porphyrin (CuC1TPP)	Paraoxon (2.5×10^{-5} μM) Diazinon (2.6×10^{-3} μM) Malathion (0.302×10^{-2} μM) Coumaphos (0.689 μM)	10^{-2}– 10^{5} ppb 1–10^{5} ppb 10–10^{4} ppb 10–10^{5} ppb	–	230 d	10 s (paraoxon)	White and Harmon (2005)
	2. *E. coli* whole cells harboring plasmid pTInaPb-N/OPH	Paraoxon (0.2 μM) Parathion (0.4 μM) Methyl parathion (1 μM)	0.5–150 μM 1–200 μM 2.5–200 μM	–	Approx. 30 d	≤10 min	Tang, Liang et al. (2014)
	3. OPH on nylon membrane connected to optical fibers	Paraoxon (2 μM) Parathion (2 μM) Coumaphos (5 μM)	0.01–0.48 mM (steady state) 0.02–0.5 mM (kinetic) 0.01–0.2 mM (steady state) 5–35 mM (kinetic)	0.0022/μM (steady state); 0.00092/min/μM (kinetic) 0.002/μM (steady state) 0.0005/min/% (kinetic)	10 d	14 min (steady state), 2 min. (kinetic)	Mulchandani, Pan, Chen (1999)
	4. MAP based adhesion	Paraoxon (5 μM)	5–320 μM	–	28 d	5 min	Kim et al. (2013)
Flavobacterium sp. MTCC 2495	1. Glass fiber filter paper	Methyl parathion (0.3 μM)	4–80 μM	–	1 month	<3 min	Kumar et al. (2006)
Sphingomonas sp. JK1	1. Glutaraldehyde as linker; direct deposition of *Spinghomonas* sp. JK1 on microplate reader wells	Methyl parathion (4 μM)	4–80 μM	–	18 d	5 min	Kumar and D'Souza (2010)
	2. Inner epidermis of onion bulb scale and glutaraldehyde	Methyl parathion (4 μM)	4–80 μM	–	32 d	5 min	Kumar and D'Souza (2011a)
3.2 Fluorometric biosensors							
E. coli	1. CdSe QDs / OPH	Paraoxon (10^{-9} mol/L)	1×10^{-8} to 1×10^{-5} mol/L	–	–	~10 min	Constantine, Gattás-Asfura et al. (2003)
	2. OPH with a histidine tail (OPH6His) bioconjugated with pyranine—with the aid of silica-coated silver nanoparticles	Paraoxon (2 ppb) Methyl parathion (10 ppb)	5–100 ppb 20–100 ppb	–	–	<3 min	Thakur et al. (2013)
	3. Fluorescein isothiocyanate covalently bound to OPH	Paraoxon (8 μM)	25–400 μM	–	90 d	–	Rogers et al. (1999)
	4. OPH-conjugated gold nano particles with 7-hydroxy-9H-(1,3-dichloro9,9-dimethylacridin-2-one(DDAOphosphate) as decoy	Paraoxon (20 μM)	0–240 μM	–	–	–	Simonian et al. (2005)
P. aeruginosa	1. OPH-conjugated gold nanoparticles with and without linking system (glutaraldehyde-cystamine) and cumarin1 as decoy	Paraoxon (5×10^{-5} μM)	50–1050 nM	–	–	–	Kamelipour et al. (2014)

(*continued*)

Table 3. Continued.

Cell type	Type (material)	Substrate (LOD)	Linear range	Sensitivity	Stability	Response time	Reference
	2. Chitosan-gold nanoparticles organophosphorus hydrolase nano bio conjugate with Coumarin1 as decoy	Paraoxon (5×10^{-5} μM)	0–1050 nM	–	21 d, 80% activity	<30 min	Karami et al. (2016)
P. diminuta	1. OPH-conjugated nano magnet-silica core-shell with coumarin 1 as decoy	Paraoxon (5×10^{-6} μM)	10–250 nM	–	–	–	Khaksarinejad et al. (2015)
	2. Fluorescent dye/OPH	Paraoxon (5×10^{-9} mol/L)	5×10^{-9} – 1×10^{5} M	–	–	30 s	Orbulescu et al. (2006); Zheng et al. (2005)
3.3 Fiber optic microbial biosensor							
E. coli	1. *E. coli* cell suspension on fiber optic sensor strip	Paraoxon (3 μM)	0.0–0.6 mM	5.98×10^{-4} min^{-1} μM^{-1}	32 d	<10 min	Mulchandani, Kaneva, Chen (1998)
		Parathion (3 μM)	0.0–0.03 mM	3.4×10^{-4} min^{-1} μM^{-1}			

spectrophotometer. The discs were inserted into the reaction medium in the presence of OP compounds, and the changes in absorbance were noted through the UV–Vis spectrophotometer. This method reported a detection limit of 0.3 μM and a linear range of 4–80 μM for methyl parathion (Table 3.1) (Kumar et al. 2006). White and Harmon developed a biosensor based on immobilization of *E. coli* expressing OPH on ProbeOn^{TM} Plus slides with gultaraldehyde as a linker and complexation with the porphyrin meso-tri(4-sulfonato phenyl) mono(4-carboxy phenyl) porphyrin (C1TPP) which is competitively bound to OPH. Upon introduction of OP compounds, the porphyrin is unbound and the reaction of OP compound with OPH generates *p*-nitrophenol, which is measured by a change in absorbance at 412 nm, through an optical fiber based UV–Vis spectrophotometer. This sensor was able to display a low detection limit of 7 ppt (25 pM) for paraoxon (Table 3.1) (White and Harmon 2005). Kim et al. developed a biosensor by immobilizing whole cells of recombinant *E. coli* expressing periplasmic OPH onto the surface of a 96-well microplate using mussel adhesive protein as a microbial cell immobilizing linker. The resultant setup was able to detect through changes in absorbance at 410 nm, paraoxon in quantities as low as 5 μM, with a linear range of 5–320 μM and good stability, 80% activity retention up to 28 d and reusability up to 20 times (Table 3.1) (Kim et al. 2013). With a view to improving the catalytic activity of substrates, researchers have investigated surface expression in cells. Tang et al. developed a sensor based on surface expression of *E. coli* bacteria expressing OPH with an anchored INP which showed detection limits of 0.2, 0.4, and 1 μM for paraoxon, parathion, and methyl parathion, respectively, based on monitoring of production of *p*-nitrophenol through absorption spectra at 410 nm, a principle that is followed for most studies in this category. The same sensor showed a broad linear range of 0.5–150 μM paraoxon, 1–200 μM parathion and 2.5–200 μM methyl parathion, respectively (Table 3.1) (Tang, Liang et al. 2014). Thus, both periplasmic and surface expressed bacteria have shown promise in achieving detection of OPs. Another approach shown to be effective for improved detection OPs, is by mineralization of cells for attachment of OPH using $Co_3(PO_4)_2.8H_2O$. Han and Liu developed a novel biosensor using $Co_3(PO_4)_2.8H_2O$ which was mineralized onto the surface of OPH fused bacteria expressing OPH. The embedding of OPH into $Co_3(PO_4)_2.8H_2O$ crystals greatly enhanced the activity through the allosteric effect. The resultant hybrids, when used as a sensor based on the change in absorbance at 410 nm in the presence of paraoxon, were found to have a detection limit of 0.08 μM and a linear range of 0.2–200 μM. Furthermore, this sensor was found to have greater recovery rates of 97–102% when used to detect paraoxon in real samples, such as seawater, tap water, and sewage water (Han and Liu 2017). In addition to the location of expression of OPH inside cells, advanced materials like nanomaterials or nanofabricated chips or solid crystals have also been described to be able to detect OPs. Kim et al. developed a MEMS chip with etched gaps between two electrodes wherein SWNT attached *E. coli* strain expressing periplasmic OPH was inserted. This chip was then attached to a "chamber" containing the analyte solution (e.g.

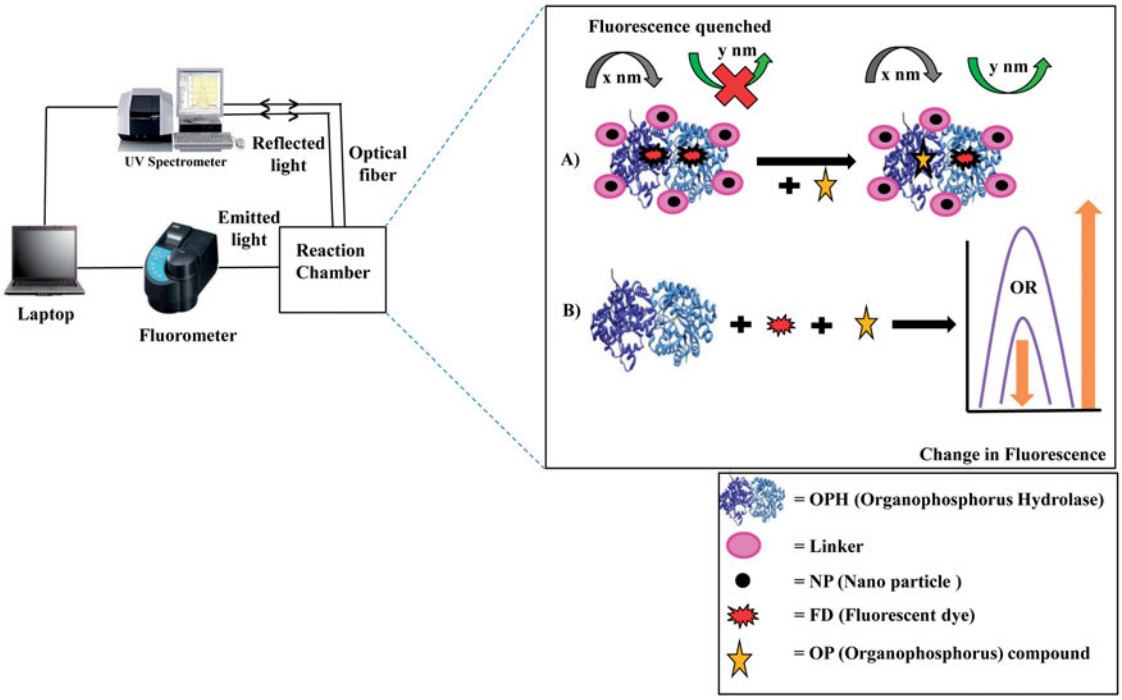

Figure 6. Schematic diagram of optical sensing system: Inset shows mechanism of fluorescence as well as spectrophotometric based sensing of OPH. (A) OPH conjugated with nanoparticle, linker and fluorescent dye does not exhibit fluorescence when excited at "x" nm, but exhibits fluorescence by emission at "y" nm when OP compound is added due to competitive binding of OP compound with OPH. (B) OPH in presence of a fluorescent dye exhibits fluorescence. On addition of OP compound, binding of OPH with OP compound may either increase or decrease the fluorescence emission.

paraoxon), and then the reaction was allowed to proceed for up to 50 min. The absorbance of the analyte solution was then measured at 400 nm to determine the effect of OPH on the OPs. The authors reported a linear range of 20–500 μM and a detection limit of 5 μM for this sensor (Kim et al. 2015).

Absorbance based sensors developed by White and Harmon using copper complexed meso-tri (4-sulfonatophenyl) mono (4-carboxyphenyl) porphyrin as a reversible inhibitor for OPH displays encouraging results in terms of detection limit (2.5×10^{-5} μM for paraoxon), linear range (10^{-2} to 10^{5} ppb), stability (~230 d), and response time (under 10 s) (White and Harmon 2005). In terms of sensitivity, the enzyme-modified fiber optic sensor developed by Mulchandani et al. displays a high sensitivity of 0.0022/μM (steady state) or 0.0092/μM (kinetic) and a linear range of 5000–35 000 μM (Mulchandani, Pan, Chen 1999). Although UV–Vis absorbance based sensing has some advantages with respect to lower costs and potential to detect additional contaminants through other specific peaks, this method has limitations of poor signal-to-noise ratio which affects the sensitivity as well as selectivity. In cases where the costs are not a concern and highly specific and selective detection is required, fluorescence sensors are often considered to be a better choice (Nemzer and Epstein 2010).

Fluorescence-based sensors

Fluorescence-based sensors are either based on the quenching of fluorescence or an increase in fluorescence intensity when an analyte is converted into a product. Interaction of OPs with OPH leads to the formation of *p*-nitrophenol with the release of protons which can very easily be linked to fluorescence-based estimation. The pH drop occurring during catalytic reaction may be linked to pH based fluorescent sensors (Chaudhari et al. 2017). Among the several methods of using OPH for detection of OPs, use of pH sensitive fluorophores like fluorescein isothiocyanate (FITC), coumarin 1, poly-thiophene-3-acetic acid (PTAA), etc., are the most common transduction mechanisms followed in the literature reports. An example of a fluorophore with pH sensitive properties is FITC which causes a depletion of fluorescence intensity as the reaction of OPH progresses. Mulchandani et al. and Roger et al. used this principle to covalently immobilize FITC to OPH, and then adsorb the FITC-labeled OPH to polymethyl methacrylate (PMMA) beads. The detection mechanism is based on the change of fluorescence due to the change in pH caused by the action of OPH on OPs, wherein existing fluorescence is quenched as a substrate for OPH (i.e. OPs) is introduced. The observed limit of detection was 8 μM for paraoxon and coumaphos, and up to 50 μM for crotoxyphos (Rogers et al. 1999; Mulchandani Chen, Mulchandani, Wang, Rogers 2001) (Table 3.2).

Another fluorescence quenching based mechanism was employed using coumarin 1 in combination with OPH by Paliwal et al. who used an excitation wavelength of 343 nm for a solution containing 1:1 coumarin 1: OPH and fluorescence quenching measured at 465 nm after addition of OPs. A detection limit of 0.7 μM was observed for paraoxon with a linear range of 1–8 μM (Paliwal et al. 2007). Coumarin 1 was also utilized as an indirect assay by Karami et al. wherein electrostatically attached Au nanoparticles were immobilized along with OPH and coumarin 1 in chitosan. The method of sensing was the change in fluorescence of coumarin 1, wherein the fluorescence was quenched in the presence of

OPH-Au nanoconjugate but was enhanced when paraoxon was introduced into the solution, due to the tendency of paraoxon to replace coumarin 1 as the substrate for OPH. The limit of detection in this study was as low as 50 pM (Table 3.2) (Karami et al. 2016). Constantine et al. developed a quartz substrate comprising of five bilayers of chitosan and PTAA on which OPH was deposited and the fluorescence spectrum of PTAA with chitosan was recorded at 575 nm (excitation wavelength 480 nm) in the absence and presence of paraoxon. The fluorescence was quenched by the presence of paraoxon and the limit of detection was found to be 1 nM (Constantine, Mello et al. 2003). Use of nanomaterials for enhancing the sensitivity of detection is a very common approach used in all the biosensors including fluorescent biosensors. Light responsive nanomaterials like gold nanoparticles, quantum dots, core-shell nanoparticles of silica etc., are very commonly employed with OPH for detection. Kamelipour et al. used glutaraldehyde-cystamine as a linker to develop a conjugate of Au nanoparticles and OPH expressed in *Pseudomonas aeruginosa* and appropriately purified to detect paraoxon in human serum. The sensing mechanism is similar to that mentioned previously, and a detection limit of 50 pM was observed (Table 3.2) (Kamelipour et al. 2014). Ji et al. designed a conjugate of OPH with (CdSe) ZnS quantum dots, and detected paraoxon using the principle of photoluminescence quenching at 570 nm with a 350 nm excitation in the presence of paraoxon, which they concluded, was caused by a secondary structure change in OPH during the interaction with paraoxon, which in this case interacts with OPH as a substrate rather than as an inhibitor. The detection limit was found to be 0.01 μM of paraoxon (Ji et al. 2005). Khaksarinejad et al. using OPH conjugated with (3-Aminopropyl)triethoxysilane (APTES) activated Fe_3O_4-SiO_2 core-shell nanoparticles wherein glutaraldehyde was used as a cross-linker. In this study, a low detection limit of 5 pM was reported (Table 3.2) (Khaksarinejad et al. 2015). The whole cell-based biosensors using OPH and fluorescence transduction mechanisms are meager in literature. In one of the fluorescent whole cell-based biosensor described by Fleischauer et al. OPH expressing *E. coli* bacteria was immobilized in a hydrogel precursor and crosslinked by adding in mineral oil and crosslinked by photopolymerization in UV light for 5 s. The fluorescence intensity of a standard solution containing a pH sensitive fluorescent dye and a standard quantity of paraoxon was recorded with and without the beads. The reaction between OPs and OPH causes an increase in acidity, changing the pH and consequently the fluorescence intensity ratio. A detection limit of 3 μM was observed for this sensor (Fleischauer and Heo 2014).

In terms of linear range and detection limit, Khaksarinejad et al. have obtained the best results for their sensor based on competitive binding of coumarin 1 to OPH, with values of 10–250 nM and 5 pM, respectively (Table 3.2) (Khaksarinejad et al. 2015). Rogers et al. have obtained an impressive linear range of 25–400 μM and good stability of 90 d in their sensor based on fluorescence signal quenching of FITC bound OPH in the presence of paraoxon, but this study falls behind in terms of the detection limit (8 μM for paraoxon) (Table 3.2) (Rogers et al. 1999). Thakur et al. have reported a fast response times of less than 3 min in their study based on metal nanoparticle enhanced fluorescence of OPH conjugated with a pyranine complex (Table 3.2) (Thakur et al. 2013). Fluorometric sensors have advantages of sensitivity. However, this method is dependent on the components and materials in the test setup, which can absorb or reflect the light and hence affect the readings. In practice, this necessitates an expensive setup and is not easily deployed in real-world scenarios and on-site detection methodology due to such limitations (Ryškevič et al. 2010).

Other methods of sensing

In addition to the methods described above, efforts have also been made toward utilizing new and upcoming principles of science toward the sensing and detection of OPs. For example, Walker et al. developed a photonic crystal-based sensing platform wherein a bimodular sensing motif was utilized in Intelligent Polymerized Crystalline Colloidal Array (IPCCA) with OPH as the first sensing material and 3-aminophenolate (3-AMP) as the second sensing material, added as functionalizing agents in the IPCCA matrix. The IPCCAs comprise of colloidal nanoparticles polymerized in a hydrogel which diffracts light in the visible spectral region. The OPH degrades methyl parathion to *p*-nitrophenol and dimethyl phosphate at pH 9.7, with two protons as a byproduct. The protons protonate the 3-AMP, causing a change in the steady-state volume in the IPCCA. This causes a change in the wavelength of diffracted light, a blue-shift, and is directly proportional to the number of protons generated, i.e. the quantity of methyl parathion. In practice, the difference was measured by the change in reflectance using a UV–Vis spectrophotometer, in contrast to the measurement of absorbance of *p*-nitrophenol in other studies concerning detection of OP compounds. A detection limit of 0.2 μM for methyl parathion was observed (Walker et al. 2007).

Magnetoelastic sensors have come up as new advanced sensors which are based on substrates made of amorphous ferromagnetic materials which vibrate when subjected to an AC (alternating current) signal. The resultant magnetic flux can be easily sensed by means of an excitation coil and an acoustic wave that can be monitored over several meters. Furthermore, one can also visualize the vibration of the magnetoelastic strip by observing the attenuation of a laser beam reflected from its surface. Zourob et al. developed a sensor based on the magnetoelastic concept wherein OPH was dropped on a pH-sensitive polymer layer coated on the top of a ribbon of a magnetoelastic material. On interaction with the target analyte, the reaction between OPH and the OP compound would induce changes in pH, causing the polymer layer to swell, which changes the density and elasticity of the composite strip comprising of a magnetoelastic material, polymer layer and OPH. The result is a change in fundamental frequency. The sensor was found to have a detection limit of 0.1 μM for paraoxon and 0.85 μM for methyl parathion, respectively (Zourob, Simonian et al. 2007).

Strategies to improve enzyme specificity, activity, and stability

Though enzymes such as OPH have great potential for developing as biosensors, their *in-vivo* functioning is quite different than that used in the laboratory and industrial settings. To improve the substrate specificity, various mutants have been created by site-directed mutagenesis in the active site of the OPH. By altering specific residues of amino acids, the electrostatic interaction between the side chain and hydrogen bond can be disrupted that decrease the affinity toward the smaller substrate and add flexibility for the larger molecules that enter into the active site (Theriot and Grunden 2011). In the rational design approach, researchers use structural data and crystal structures to identify portions of a compound that may be mutated specifically to obtain certain designed characteristics. Alternatively, in the directed evolution approach, libraries of mutant genes are created through means of gene recombination and/or random mutagenesis. These mutant genes are cloned into expression vectors and inserted into microbes for protein expression. The expressed proteins are then identified and screened to be used as templates for next rounds of development (Johannes and Zhao 2006). Both rational design and directed evolution approaches have been used in contemporary literature to try and improve the specificity, activity, and stability of OPH.

Schofield and DiNovo created 8 OPH mutants using site-directed mutagenesis, displaying immensely improved activity for the degradation of demeton s-methyl with a 24 times improvement in specificity and established a correlation between enzymatic activity for demeton s-methyl degradation and VX (Schofield and DiNovo 2010). Similarly, Gopal et al. described a rationally designed L136Y mutant of OPH, based on similarities in structure to AChE, which displayed a 33% increase in hydrolysis rates of VX compared to the wild-type enzyme (Gopal et al. 2000). On the similar lines, Reeves et al. also created a number of mutants, two of which displayed 10 and 39 times greater activity for the degradation of VX compared to the wild-type enzyme. They postulated that substitutions of histidines at the 254th and 257th position in the wild-type OPH with arginine and phenylalanine residues, respectively, have a significant impact on the catalytic activity toward hydrolysis of P—S bonds, bringing the best balance between higher catalytic activity and uncompromised stability (Reeves et al. 2008). On the other hand, Jeong et al. used a rational design based on substrate docking simulation and studies on the structure of OPH to design a double mutant L271/Y309A which delivered a striking 150 fold increase in catalytic efficiency for VX compared to wild-type protein (Tokuriki and Tawfik 2009).

To enhance the protein expression at the cell surface, Cho et al. altered the OPH enzyme obtained from *P. diminuta* to include a truncated ice nucleation motif, in which the mutagenized variants were screened by checking for hydrolysis activity and production of a byproduct, *p*-nitrophenol. The first study yielded an enzyme 22A11, which was found to break down methyl parathion 25 times faster than wild-type OPH (Cho et al. 2002). This variant was then used as a template in directed evolution to create a new variant (Cho et al. 2004) B3561, which was able to hydrolyze chlorpyrifos at a rate of 750 times greater than wild-type OPH. It was also observed that these variants were able to perform faster hydrolysis of parathion and its metabolic byproduct, paraoxon. These studies identified three key mutations that affected the hydrolysis activity of OPH – A80V, I274N, and K185R. The other substitutions found in variants 22A11 and B3561 had led Cho et al. to believe that conformational changes led to a wider active site, which improved catalytic turnover and efficiency (Mee-Hie Cho et al. 2006). Naqvi et al. described a variant of OPH from *Agrobacterium radiobacter* with S308L/T309A substitutions in the substrate binding pocket, which displayed over 5000 fold increase in activity toward degradation of malathion. They confirmed that widening of the active site of OPH was responsible for the enhanced activity (Naqvi et al. 2014).

Cherny et al. used iterative computational modeling to design variants of OPH which resulted in a 5000-fold increase in catalytic efficiency for detoxification of V-series of nerve agents (VE, VG, VM, VR, and VX) and also was effective for detoxification of G-series of nerve agents (GA, GB, GD, GF, and GV) (Cherny et al. 2013). In another study, diSioudi et al. replaced the histidine at position 254 with arginine (H254R) and the one at position 257 with leucine (H257L) independently, as well as double mutation (H254R/H257L) in OPH enzyme. Interestingly, these mutants of OPH possessed only two metals per dimer, as compared to four per dimer in native OPH. All three of these altered enzymes demonstrated a 2–30-fold increase in substrate specificity (kcat/Km) for demeton S (P—S bond), an analog for the chemical warfare agent VX. Furthermore, two of the altered enzymes, H257L and H254R/H257L, showed an 11- and 18-fold increase, respectively, in specificity for NPPMP, the analog for the chemical warfare agent soman (diSioudi et al. 1999).

Interestingly, to increase the solubility of OPH, Tokuriki et al. expressed OPH in a strain in which chaperonins is overexpressed, as they assist in the proper folding of proteins. Their experiments showed that OPH solubility is 2.4 times enhanced in the presence of overexpressed chaperonins. Similarly, a few novel cloning strategies were explored to express OPH on the cell surface to increase its access to the substrate and thereby enhancement in its activity (Tokuriki and Tawfik 2009). Toward this approach, a new anchor system based on the INP from *Pseudomonas syringae* INA5, was employed to display functional OPH on the cell surface of *Moraxella* sp. The OPH activity for this new cell was reported to be 80-fold higher than in *E. coli* and thus offers a potential for greatly improved biosensor performance (Mulchandani, Chen, Mulchandani, Wang, Chen 2001).

Discussion and future prospects

There is an urgent need to develop low-cost, fast, and easy to use sensing devices for detection of OPs. According to the medical studies performed on the people who are significantly exposed to OP compounds, the blood concentrations of OPs in are in the range of 65.71 nM (Wagner and Orwick 1994; Huen et al. 2012), 0.2–0.89 μM (Fournier et al. 1978),

0.3993 μM, and 1.25 μM (Isbister et al. 2007) for diazinon, parathion, chlorpyrifos, and methyl parathion, respectively, and therefore, a sensor must be able to detect such low concentrations in complex samples, so that they can be considered ready for deployment as a point-of-care device. In this respect, the best success so far has been achieved for methyl parathion and parathion using electrochemical sensors, while sensors for other organophosphates still have not reached the desired levels of detection and sensitivity required for the commercial grade standardization and testing. Although various methods of sensing have been described here, many of them have several limitations. Several studies have investigated OPH from different organisms, better results have been obtained using *P. putida* strains instead, with a 67% higher threshold (1000 μM) of *p*-nitrophenol concentration for complete activity inhibition compared to *E. coli* strains (600 μM) (Gilbert et al. 2003). Electrochemical methods have recorded broader values for linear range, e.g. 0.05–25 μM (Tang, Zhang et al. 2014) and sensitivity, 198 nA/μM (Lee et al. 2010). Further improvements in the activity and stability may be pursued by encapsulation of OPH enzyme as well as by the use of synergistic effect with nanoparticle systems. In this respect, efforts toward increasing the activity and kinetics of OP degradation can be of great importance toward enhancing the sensitivity, limit of detection, and stability of biosensors. While electrochemical and optical methods have attracted similar amounts of attention, among the reported investigations, optical methods appear to have an edge with lower limits of detection better stability and lower response time. For example, White et al. observed values of 2.5×10^{-5} μM, 230 d and 10 s for the detection limit, stability and response time, respectively using a UV–visible spectrometric biosensor (White and Harmon 2005). Another picomolar level detection was obtained using a coumarin 1 decoy based OPH (obtained from *P. diminuta*) conjugated core-shell nanoparticles (Khaksarinejad et al. 2015). However, the inherent dependence of UV–visible and fluorescence spectra on the concentration of the substrates and/or enzyme in a liquid medium creates several concerns over repeatability of the tests owing to the transient nature of concentration of solutes in real-world scenarios like lakes, rivers, etc. Electrochemical techniques against their expectations have been able to detect at levels only till nM levels of OPs only in comparison to the optical counterparts. This nM limit of detection has been achieved in case of OPH derived from *P. putida* using a carbon paste electrode in an electrochemical cell. Improved detection in LOD values for paraoxon, methyl parathion, parathion, thiobenzene phosphonate, and fenitrothion detection have been described in the range of 1–5 nM. However, in this case, the stability of the developed sensor is only 5 d which can be improved to a great extent. Use of conducting polymers and conducting nanomaterials in electrochemical OPH biosensors could further bring the LOD values to sub-picomolar levels which are highly essential considering the toxicity of OPs.

In addition to their application in developing biosensors, these OP degrading enzymes have tremendous potential in bioremediation of hazardous OPs. The currently used methods for the degradation of OPs include two main categories, enzymatic mode of degradation and non-enzymatic mode of degradation. Non-enzymatic mode of degradation can be further divided into a chemical and physical mode of degradation. Using the physical mode one can flush the contaminants away but cannot destroy them (Jacquet et al. 2016). Eradication of contaminants using physical methods relies on the basic principle of removal and absorption from the surface. Chemical mode of degradation includes all the methods like oxidation, reduction, and hydrolysis which allow the neutralization of the OPs. But these methods are often toxic, allergic and cause damage to the environment as well as humans. Thus, there is a need for the development of the method by which OPs can be hydrolyzed without causing any harm and with broad substrate specificity, inciting interest in the use of enzymes for this purpose, such as MPH or OPH. In fact, Bai et al. developed a *Pichia pastoris* strain expressing an engineered variant PoOPHM9. The enzyme obtained from this strain degraded 0.15 mM of malathion in only 5 min with only 0.04 mg/mL of the enzyme (Bai et al. 2017). This is the fastest degradation time reported in contemporary literature, with other reports stating degradation times in hours or days (Lei, Mulchandani, Chen 2005; Seo et al. 2007).

Toward developing robust biosensors for the detection of OPs, future research must focus on enhancing the limits of detection and sensitivity of the sensors. One approach of achieving this could be by choosing a recombinant OPH with improved sensitivity, specificity, and stability in high efficiency matrices investigated in this review. Moreover, they can be coupled with methods which offer enhanced convenience of measurement that deliver an electrical or optical output. Methods based on optical fibers and magneto-elastic films are particularly attractive from the point-of-view of compact devices for portable and fast detection and analysis of real samples, such as water and/or blood. Reports of OP compound detection in blood/serum or human samples are meager in the literature, however, human serum paraoxonase 1 can be used for the detection of nerve agents as it has shown potential for degradation of nerve agent VX (Peterson et al. 2011). Several advanced techniques of biosensing like surface plasmon resonance, piezoelectric, chemiluminescence, surface-enhanced Raman spectroscopy, etc. are still to be investigated utilizing OPH. Fiber optic systems provide excellent alternatives for portability of UV–Vis or fluorescence measurement using chromophore/fluorophore linked OPH based OPs detection. Several configurations of free enzyme, immobilized enzymes, free cells or immobilized cells can be put to test using these fiber optic systems. Nanomaterials, films, mesoporous materials, modified electrodes, quantum dots, molecularly imprinted polymers, and aptamer-based detection such other advanced materials can also be used for immobilization or improving the biosensor performance, toward the development of point-of-care devices for real-time analysis.

Acknowledgments

P. Kodgire and A. Joshi thanks Department of Biotechnology, Govt. of India, for research grants (BT/PR20319/BBE/117/189/2016 and

BT/PR24652/NER/95/795/2017). A. Joshi would like to thank SERB-ECR and DST-INSPIRE faculty award. M. Jain thanks the Ministry of Human Recourse Development (MHRD), Government of India, for PhD fellowship. The authors gratefully acknowledge the constructive comments of the reviewers who were selected by the Editor and anonymous to the authors.

Declaration of interest

The authors' affiliations are as shown on the cover page. The authors declare no competing financial interests. The study was mainly financed by the above-mentioned research grants. Preparation of this review was conducted during the normal course of the author's employment without external influence or support other than the referred grants. The review is the professional work product of the authors and the views expressed are not necessarily the views of their employers. None of the authors have appeared during the last five years in any regulatory or legal proceedings related to the contents of this paper.

References

Abou-Donia MB. 1995. Involvement of cytoskeletal proteins in the mechanisms of organophosphorus ester-induced delayed neurotoxicity. Clin Exp Pharmacol Physiol. 22:358–359.

Amitai G, Gaidukov L, Adani R, Yishay S, Yacov G, Kushnir M, Teitlboim S, Lindenbaum M, Bel P, Khersonsky O, et al. 2006. Enhanced stereoselective hydrolysis of toxic organophosphates by directly evolved variants of mammalian serum paraoxonase. FEBS J. 273:1906–1919.

Atwood D, Paisley-Jones C. 2017. Pesticides industry sales and usage: 2008–2012 market estimates. Washington (DC): United States Environmental Protection Agency.

Bai YP, Luo XJ, Zhao YL, Li CX, Xu DS, Xu JH. 2017. Efficient degradation of malathion in the presence of detergents using an engineered organophosphorus hydrolase highly expressed by *Pichia pastoris* without methanol induction. J Agric Food Chem. 65:9094–9100.

Barak D, Ordentlich A, Segall Y, Velan B, Benschop HP, De Jong LP, Shafferman A. 1997. Carbocation-mediated processes in biocatalysts. Contribution of aromatic moieties. J Am Chem Soc. 119:3157–3158.

Barr JR, Driskell WJ, Aston LS, Martinez RA. 2004. Quantitation of metabolites of the nerve agents sarin, soman, cyclohexylsarin, VX, and Russian VX in human urine using isotope-dilution gas chromatography-tandem mass spectrometry. J Anal Toxicol. 28:372–378.

Benning MM, Shim H, Raushel FM, Holden HM. 2001. High resolution X-ray structures of different metal-substituted forms of phosphotriesterase from *Pseudomonas diminuta*. Biochemistry. 40:2712–2722.

Bigley AN, Raushel FM. 2013. Catalytic mechanisms for phosphotriesterases. Biochim Biophys Acta Proteins Proteomics. 1834:443–453.

Chaudhari R, Joshi A, Srivastava R. 2017. pH and urea estimation in urine samples using single fluorophore and ratiometric fluorescent biosensors. Sci Rep. 7:5840.

Cherny I, Greisen P Jr Ashani Y, Khare SD, Oberdorfer G, Leader H, Baker D, Tawfik DS. 2013. Engineering V-type nerve agents detoxifying enzymes using computationally focused libraries. ACS Chem Biol. 8: 2394–2403.

Cho CH, Mulchandani A, Chen W. 2002. Bacterial cell surface display of organophosphorus hydrolase for selective screening of improved hydrolysis of organophosphate nerve agents. Appl Environ Microbiol. 68:2026–2030.

Cho CH, Mulchandani A, Chen W. 2004. Altering the substrate specificity of organophosphorus hydrolase for enhanced hydrolysis of chlorpyrifos. Appl Environ Microbiol. 70:4681–4685.

Chough SH, Mulchandani A, Mulchandani P, Chen W, Wang J, Rogers KR. 2002. Organophosphorus hydrolase-based amperometric sensor: modulation of sensitivity and substrate selectivity. Electroanalysis. 14: 273–276.

Chu X, Zhang X, Chen Y, Liu H, Song D. 2003. Study on the properties of methyl parathion hydrolase from Pseudomonas sp. WBC-3. Wei Sheng Wu Xue Bao. 43:453–459.

Constantine CA, Gattás-Asfura KM, Mello SV, Crespo G, Rastogi V, Cheng TC, DeFrank JJ, Leblanc RM. 2003. Layer-by-layer biosensor assembly incorporating functionalized quantum dots. Langmuir. 19:9863–9867.

Constantine CA, Mello SV, Dupont A, Cao X, Santos D, Oliveira ON, Strixino FT, Pereira EC, Cheng TC, Defrank JJ, et al. 2003. Layer-by-layer self-assembled chitosan/poly(thiophene-3-acetic acid) and organophosphorus hydrolase multilayers. J Am Chem Soc. 125: 1805–1809.

Daczkowski CM, Pegan SD, Harvey SP. 2015. Engineering the organophosphorus acid anhydrolase enzyme for increased catalytic efficiency and broadened stereospecificity on Russian VX. Biochemistry. 54: 6423–6433.

Deo RP, Wang J, Block I, Mulchandani A, Joshi KA, Trojanowicz M, Scholz F, Chen W, Lin Y. 2005. Determination of organophosphate pesticides at a carbon nanotube/organophosphorus hydrolase electrochemical biosensor. Anal Chim Acta. 530:185–189.

Di Sioudi BD, Miller CE, Lai K, Grimsley JK, Wild JR. 1999. Rational design of organophosphorus hydrolase for altered substrate specificities. Chem Biol Interact. 119:211–223.

Di Sioudi B, Grimsley JK, Lai K, Wild JR. 1999. Modification of near active site residues in organophosphorus hydrolase reduces metal stoichiometry and alters substrate specificity. Biochemistry. 38:2866–2872.

Donaldson D, Kiely T, Grube A. 1997. Pesticide's industry sales and usage 1998–1999 market estimates. US Environmental Protection Agency; Washington (DC): Report No. EPA-733-R-02-OOI. Available from: http://www.epa.gov/oppbead/pesticides/99 pestsales/market-estimates. pdf.

Dong YJ, Bartlam M, Sun L, Zhou YF, Zhang ZP, Zhang CG, Rao Z, Zhang XE. 2005. Crystal structure of methyl parathion hydrolase from Pseudomonas sp. WBC-3. J Mol Biol. 353:655–663.

Du D, Chen W, Zhang W, Liu D, Li H, Lin Y. 2010. Covalent coupling of organophosphorus hydrolase loaded quantum dots to carbon nanotube/Au nanocomposite for enhanced detection of methyl parathion. Biosens Bioelectron. 25:1370–1375.

Duysen EG, Li B, Xie W, Schopfer LM, Anderson RS, Broomfield CA, Lockridge O. 2001. Evidence for nonacetylcholinesterase targets of organophosphorus nerve agent: supersensitivity of acetylcholinesterase knockout mouse to VX lethality. J Pharmacol Exp Ther. 299: 528–535.

Eddleston M, Buckley NA, Eyer P, Dawson AH. 2008. Management of acute organophosphorus pesticide poisoning. Lancet. 371:597–607.

Eddleston M. 2000. Patterns and problems of deliberate self-poisoning in the developing world. QJM. 93:715–731.

Farnoosh G, Latifi AM. 2014. A review on engineering of organophosphorus hydrolase (OPH) enzyme. J Appl Biotechnol Rep. 1:1–10.

Fleischauer V, Heo J. 2014. An organophosphate sensor based on photocrosslinked hydrogel-entrapped *E. coli*. Anal Sci. 30:937–942.

Fournier E, Sonnier M, Dally S. 1978. Detection and assay of organophosphate pesticides in human blood by gas chromatography. Clin Toxicol. 12:457–462.

Fukuto TR. 1990. Mechanism of action of organophosphorus and carbamate insecticides. Environ Health Perspect. 87:245.

Gäberlein S, Knoll M, Spener F, Zaborosch C. 2000. Disposable potentiometric enzyme sensor for direct determination of organophosphorus insecticides. Analyst. 125:2274–2279.

Ghanem E, Raushel FM. 2005. Detoxification of organophosphate nerve agents by bacterial phosphotriesterase. Toxicol Appl Pharmacol. 207: 459–470.

Gilbert E, Walker A, Keasling J. 2003. A constructed microbial consortium for biodegradation of the organophosphorus insecticide parathion. Appl Microbiol Biotechnol. 61:77–81.

Gopal S, Rastogi V, Ashman W, Mulbry W. 2000. Mutagenesis of organophosphorus hydrolase to enhance hydrolysis of the nerve agent VX. Biochem Biophys Res Commun. 279:516–519.

Gothwal A, Beniwal P, Dhull V, Hooda V. 2014. Preparation of electrochemical biosensor for detection of organophosphorus pesticides. Int J Anal Chem. 2014:1.

Graham SC, Bond CS, Freeman HC, Guss JM. 2005. Structural and functional implications of metal ion selection in aminopeptidase P, a metalloprotease with a dinuclear metal center. Biochemistry. 44: 13820–13836.

Guo JX, Wu JJQ, Wright JB, Lushington GH. 2006. Mechanistic insight into acetylcholinesterase inhibition and acute toxicity of organophosphorus compounds: a molecular modeling study. Chem Res Toxicol. 19:209–216.

Han L, Liu A. 2017. Novel cell-inorganic hybrid catalytic interfaces with enhanced enzymatic activity and stability for sensitive biosensing of paraoxon. ACS Appl Mater Interfaces. 9:6894–6901.

Harel M, Aharoni A, Gaidukov L, Brumshtein B, Khersonsky O, Meged R, Dvir H, Ravelli RBG, McCarthy A, Toker L, et al. 2004. Structure and evolution of the serum paraoxonase family of detoxifying and antiatherosclerotic enzymes. Nat Struct Mol Biol. 11:412.

Hartleib J, Rüterjans H. 2001. Insights into the reaction mechanism of the diisopropyl fluorophosphatase from Loligo vulgaris by means of kinetic studies, chemical modification and site-directed mutagenesis. Biochim Biophys Acta Protein Struct Mol Enzymol. 1546:312–324.

Headley DB. 1982. Effects of atropine sulfate and pralidoxime chloride on visual, physiological, performance, subjective, and cognitive variables in man: a review. Mil Med. 147:122–133.

Huen K, Bradman A, Harley K, Yousefi P, Barr DB, Eskenazi B, Holland N. 2012. Organophosphate pesticide levels in blood and urine of women and newborns living in an agricultural community. Environ Res. 117: 8–16.

Isbister GK, Mills K, Friberg LE, Hodge M, O'Connor E, Patel R, Abeyewardene M, Eddleston M. 2007. Human methyl parathion poisoning. Clin Toxicol. 45:956–960.

Jacquet P, Daudé D, Bzdrenga J, Masson P, Elias M, Chabrière E. 2016. Current and emerging strategies for organophosphate decontamination: special focus on hyperstable enzymes. Environ Sci Pollut Res Int. 23:8200–8218.

Jao SC, Huang LF, Tao YS, Li WS. 2004. Hydrolysis of organophosphate triesters by *Escherichia coli* aminopeptidase P. J Mol Catal B Enzym. 27:7–12.

Ji X, Zheng J, Xu J, Rastogi VK, Cheng TC, DeFrank JJ, Leblanc RM. 2005. (CdSe)ZnS quantum dots and organophosphorus hydrolase bioconjugate as biosensors for detection of paraoxon. J Phys Chem B. 109: 3793–3799.

Johannes TW, Zhao H. 2006. Directed evolution of enzymes and biosynthetic pathways. Curr Opin Microbiol. 9:261–267.

Kamelipour N, Mohsenifar A, Tabatabaei M, Rahmani-Cherati T, Khoshnevisan K, Allameh A, Milani MM, Najavand S, Etemadikia B. 2014. Fluorometric determination of paraoxon in human serum using a gold nanoparticle-immobilized organophosphorus hydrolase and coumarin 1 as a competitive inhibitor. Microchim Acta. 181:239–248.

Karami R, Mohsenifar A, Mesbah Namini SM, Kamelipour N, Rahmani-Cherati T, Roodbar Shojaei T, Tabatabaei M. 2016. A novel nanobiosensor for the detection of paraoxon using chitosan-embedded organophosphorus hydrolase immobilized on Au nanoparticles. Prep Biochem Biotechnol. 46:559–566.

Karpouzas DG, Singh BK. 2006. Microbial degradation of organophosphorus xenobiotics: metabolic pathways and molecular basis. Adv Microb Physiol. 51:119–225.

Katsemi V, Lücke C, Koepke J, Löhr F, Maurer S, Fritzsch G, Rüterjans H. 2005. Mutational and structural studies of the diisopropylfluorophosphatase from Loligo vulgaris shed new light on the catalytic mechanism of the enzyme. Biochemistry. 44:9022–9033.

Khaksarinejad R, Mohsenifar A, Rahmani-Cherati T, Karami R, Tabatabaei M. 2015. An organophosphorus hydrolase-based biosensor for direct detection of paraoxon using silica-coated magnetic nanoparticles. Appl Biochem Biotechnol. 176:359–371.

Kim CS, Choi BH, Seo JH, Lim G, Cha HJ. 2013. Mussel adhesive protein-based whole cell array biosensor for detection of organophosphorus compounds. Biosens Bioelectron. 41:199–204.

Kim I, Kim GH, Kim CS, Cha HJ, Lim G. 2015. Optical detection of paraoxon using single-walled carbon nanotube films with attached organophosphorus hydrolase-expressed *Escherichia coli*. Sensors. 15: 12513–12525.

Kumar J, D'Souza S. 2010. An optical microbial biosensor for detection of methyl parathion using *Sphingomonas* sp. immobilized on microplate as a reusable biocomponent. Biosens Bioelectron. 26:1292–1296.

Kumar J, D'Souza S. 2011a. Immobilization of microbial cells on inner epidermis of onion bulb scale for biosensor application. Biosens Bioelectron. 26:4399–4404.

Kumar J, D'Souza S. 2011b. Microbial biosensor for detection of methyl parathion using screen printed carbon electrode and cyclic voltammetry. Biosens Bioelectron. 26:4289–4293.

Kumar J, Jha SK, D'Souza S. 2006. Optical microbial biosensor for detection of methyl parathion pesticide using *Flavobacterium* sp. whole cells adsorbed on glass fiber filters as disposable biocomponent. Biosens Bioelectron. 21:2100–2105.

Lee JH, Park JY, Min K, Cha HJ, Choi SS, Yoo YJ. 2010. A novel organophosphorus hydrolase-based biosensor using mesoporous carbons and carbon black for the detection of organophosphate nerve agents. Biosens Bioelectron. 25:1566–1570.

Lei C, Valenta MM, Saripalli KP, Ackerman EJ. 2007. Biosensing paraoxon in simulated environmental samples by immobilized organophosphorus hydrolase in functionalized mesoporous silica. J Environ Qual. 36:233–238.

Lei Y, Mulchandani A, Chen W. 2005. Improved degradation of organophosphorus nerve agents and p-nitrophenol by *Pseudomonas putida* JS444 with surface-expressed organophosphorus hydrolase. Biotechnol Prog. 21:678–681.

Lei Y, Mulchandani P, Chen W, Mulchandani A. 2005. Direct determination of p-nitrophenyl substituent organophosphorus nerve agents using a recombinant *Pseudomonas putida* JS444-modified Clark oxygen electrode. J Agric Food Chem. 53:524–527.

Lei Y, Mulchandani P, Chen W, Mulchandani A. 2006. Biosensor for direct determination of fenitrothion and EPN using recombinant *Pseudomonas putida* JS444 with surface expressed organophosphorus hydrolase. 1. Modified Clark oxygen electrode. Sensors. 6:466–472.

Lei Y, Mulchandani P, Chen W, Mulchandani A. 2007. Biosensor for direct determination of fenitrothion and EPN using recombinant *Pseudomonas putida* JS444 with surface-expressed organophosphorous hydrolase. 2. Modified carbon paste electrode. Appl Biochem Biotechnol. 136:243–250.

Lei Y, Mulchandani P, Chen W, Wang J, Mulchandani A. 2004. Whole cell-enzyme hybrid amperometric biosensor for direct determination of organophosphorous nerve agents with p-nitrophenyl substituent. Biotechnol Bioeng. 85:706–713.

Lei Y, Mulchandani P, Wang J, Chen W, Mulchandani A. 2005. Highly sensitive and selective amperometric microbial biosensor for direct determination of p-nitrophenyl-substituted organophosphate nerve agents. Environ Sci Technol. 39:8853–8857.

Liu N, Cai X, Lei Y, Zhang Q, Chan-Park MB, Li C, Chen W, Mulchandani A. 2007. Single-walled carbon nanotube based real-time organophosphate detector. Electroanalysis. 19:616–619.

Liu FY, Hong MZ, Liu DM, Li YW, Shou PS, Yan H, Shi GQ. 2007. Biodegradation of methyl parathion by Acinetobacter radioresistens USTB-04. J Environ Sci (China). 19(10):1257–1260.

Maheshwari DT, Thygaraj V, Kumar NS. 2017. Extraction and purification of organophosphorus hydrolase enzyme from soil microorganism *Pseudomonas diminuta*. Def Life Sci J. 2:416–421.

Masson P, Josse D, Lockridge O, Viguié N, Taupin C, Buhler C. 1998. Enzymes hydrolyzing organophosphates as potential catalytic scavengers against organophosphate poisoning. J Physiol Paris. 92: 357–362.

Masson P, Nachon F, Lockridge O. 2010. Structural approach to the aging of phosphylated cholinesterases. Chem Biol Interact. 187:157–162.

Mee-Hie Cho C, Mulchandani A, Chen W. 2006. Functional analysis of organophosphorus hydrolase variants with high degradation activity towards organophosphate pesticides. Protein Eng Des Sel. 19:99–105.

Mishra RK, Barfidokht A, Karajic A, Sempionatto JR, Wang J, Wang J. 2018. Wearable potentiometric tattoo biosensor for on-body detection of G-type nerve agents simulants. Sens Actuators B Chem. 273: 966–972.

Mishra RK, Hubble LJ, Martín A, Kumar R, Barfidokht A, Kim J, Musameh MM, Kyratzis IL, Wang J. 2017. Wearable flexible and stretchable glove biosensor for on-site detection of organophosphorus chemical threats. ACS Sens. 2:553–561.

Mishra RK, Vinu Mohan AM, Soto F, Chrostowski R, Wang J. 2017. A microneedle biosensor for minimally-invasive transdermal detection of nerve agents. Analyst. 142:918–924.

Monroe D. 1989. Potentiometric (bioselective electrodes) assay systems: utility and limitations. Crit Rev Clin Lab Sci. 27:109–158.

Mulchandani A, Chen W, Mulchandani P, Wang J, Rogers KR. 2001. Biosensors for direct determination of organophosphate pesticides. Biosens Bioelectron. 16:225–230.

Mulchandani A, Kaneva I, Chen W. 1998. Biosensor for direct determination of organophosphate nerve agents using recombinant *Escherichia coli* with surface-expressed organophosphorus hydrolase. 2. Fiber-optic microbial biosensor. Anal Chem. 70:5042–5046.

Mulchandani A, Mulchandani P, Chauhan S, Kaneva I, Chen W. 1998. A potentiometric microbial biosensor for direct determination of organophosphate nerve agents. Electroanalysis. 10:733–737.

Mulchandani A, Mulchandani P, Chen W, Wang J, Chen L. 1999. Amperometric thick-film strip electrodes for monitoring organophosphate nerve agents based on immobilized organophosphorus hydrolase. Anal Chem. 71:2246–2249.

Mulchandani A, Mulchandani P, Kaneva I, Chen W. 1998. Biosensor for direct determination of organophosphate nerve agents using recombinant *Escherichia coli* with surface-expressed organophosphorus hydrolase. 1. Potentiometric microbial electrode. Anal Chem. 70: 4140–4145.

Mulchandani A, Pan S, Chen W. 1999. Fiber-optic enzyme biosensor for direct determination of organophosphate nerve agents. Biotechnol Prog. 15:130–134.

Mulchandani P, Chen W, Mulchandani A, Wang J, Chen L. 2001. Amperometric microbial biosensor for direct determination of organophosphate pesticides using recombinant microorganism with surface expressed organophosphorus hydrolase. Biosens Bioelectron. 16: 433–437.

Mulchandani P, Chen W, Mulchandani A. 2006. Microbial biosensor for direct determination of nitrophenyl-substituted organophosphate nerve agents using genetically engineered *Moraxella* sp. Anal Chim Acta. 568:217–221.

Mulchandani P, Mulchandani A, Kaneva I, Chen W. 1999. Biosensor for direct determination of organophosphate nerve agents. 1. Potentiometric enzyme electrode. Biosens Bioelectron. 14:77–85.

Muley A, Shah C, Lakhani J, Bapna M, Mehta J. 2014. To identify morbidity and mortality predictors in acute organophosphate poisoning. Indian J Crit Care Med. 18:297.

Mulyasuryani A, Prasetyawan S. 2015. Organophosphate hydrolase in conductometric biosensor for the detection of organophosphate pesticides. Anal Chem Insights. 10:23–27.

Muratova IS, Kartsova LA, Mikhelson KN. 2015. Voltammetric *vs*. potentiometric sensing of dopamine: advantages and disadvantages, novel cell designs, fundamental limitations and promising options. Sens Actuators B Chem. 207:900–906.

Naqvi T, Warden AC, French N, Sugrue E, Carr PD, Jackson CJ, Scott C. 2014. A 5000-fold increase in the specificity of a bacterial phosphotriesterase for malathion through combinatorial active site mutagenesis. PLoS One. 9:e94177.

Nath I, Chakraborty J, Verpoort F. 2016. Metal organic frameworks mimicking natural enzymes: a structural and functional analogy. Chem Soc Rev. 45:4127–4170.

Nemzer LR, Epstein AJ. 2010. A polyaniline-based optical biosensing platform using an entrapped oxidoreductase enzyme. Sens Actuators B Chem. 150:376–383.

Orbulescu J, Constantine CA, Rastogi VK, Shah SS, DeFrank JJ, Leblanc RM. 2006. Detection of organophosphorus compounds by covalently immobilized organophosphorus hydrolase. Anal Chem. 78:7016–7021.

Paliwal S, Wales M, Good T, Grimsley J, Wild J, Simonian A. 2007. Fluorescence-based sensing of p-nitrophenol and p-nitrophenyl substituent organophosphates. Anal Chim Acta. 596:9–15.

Paraíba LC, Castro V, Maia A. 2009. Insecticide distribution model in human tissues viewing worker's health monitoring programs. Braz Arch Biol Technol. 52:875–881.

Pedrosa VA, Paliwal S, Balasubramanian S, Nepal D, Davis V, Wild J, Ramanculov E, Simonian A. 2010. Enhanced stability of enzyme organophosphate hydrolase interfaced on the carbon nanotubes. Colloids Surf B Biointerfaces. 77:69–74.

Peterson MW, Fairchild SZ, Otto TC, Mohtashemi M, Cerasoli DM, Chang WE. 2011. VX hydrolysis by human serum paraoxonase 1: a comparison of experimental and computational results. PLoS One. 6:e20335.

Quinn DM, Topczewski J, Yasapala N, Lodge A. 2017. Why is aged acetylcholinesterase so difficult to reactivate? Molecules. 22:1464.

Rainina E, Efremenco E, Varfolomeyev S, Simonian A, Wild J. 1996. The development of a new biosensor based on recombinant *E. coli* for the direct detection of organophosphorus neurotoxins. Biosens Bioelectron. 11:991–1000.

Raushel FM, Holden HM. 2000. Phosphotriesterase: an enzyme in search of its natural substrate. Adv Enzymol Relat Areas Mol Biol. 74:51–93.

Raushel FM. 2002. Bacterial detoxification of organophosphate nerve agents. Curr Opin Microbiol. 5:288–295.

Reeves T, Wales M, Grimsley J, Li P, Cerasoli D, Wild J. 2008. Balancing the stability and the catalytic specificities of OP hydrolases with enhanced V-agent activities. Protein Eng Des Sel. 21:405–412.

Rogers K, Wang Y, Mulchandani A, Mulchandani P, Chen W. 1999. Organophosphorus hydrolase-based assay for organophosphate pesticides. Biotechnol Prog. 15:517–521.

Ryškevič N, Juršėnas S, Vitta P, Bakienė E, Gaska R, Žukauskas A. 2010. Concept design of a UV light-emitting diode based fluorescence sensor for real-time bioparticle detection. Sens Actuators B Chem. 148: 371–378.

Sahin A, Dooley K, Cropek DM, West AC, Banta S. 2011. A dual enzyme electrochemical assay for the detection of organophosphorus compounds using organophosphorus hydrolase and horseradish peroxidase. Sens Actuators B Chem. 158:353–360.

Scharff EI, Koepke J, Fritzsch G, Lücke C, Rüterjans H. 2001. Crystal structure of diisopropylfluorophosphatase from *Loligo vulgaris*. Structure. 9: 493–502.

Scharff EI, Lücke C, Fritzsch G, Koepke J, Hartleib J, Dierl S, Rüterjans H. 2001. Crystallization and preliminary X-ray crystallographic analysis of DFPase from *Loligo vulgaris*. Acta Crystallogr D Biol Crystallogr. 57: 148–149.

Schofield D, DiNovo A. 2010. Generation of a mutagenized organophosphorus hydrolase for the biodegradation of the organophosphate pesticides malathion and demeton-S. J Appl Microbiol. 109:548–557.

Schöning MJ, Krause R, Block K, Musahmeh M, Mulchandani A, Wang J. 2003. A dual amperometric/potentiometric FIA-based biosensor for the distinctive detection of organophosphorus pesticides. Sens Actuators B Chem. 95:291–296.

Sempionatto JR, Mishra RK, Martín A, Tang G, Nakagawa T, Lu X, Campbell AS, Lyu KM, Wang J. 2017. Wearable ring-based sensing platform for detecting chemical threats. ACS Sens. 2:1531–1538.

Seo JS, Keum YS, Harada RM, Li QX. 2007. Isolation and characterization of bacteria capable of degrading polycyclic aromatic hydrocarbons (PAHs) and organophosphorus pesticides from PAH-contaminated soil in Hilo, Hawaii. J Agric Food Chem. 55:5383–5389.

Siddavattam D. 2017. Evolution of phosphotriesterases (PTEs): how bacteria can acquire new degradative functions? Proc Indian Natl Sci Acad. 83:865–875.

Simonian A, Good T, Wang SS, Wild J. 2005. Nanoparticle-based optical biosensors for the direct detection of organophosphate chemical warfare agents and pesticides. Anal Chim Acta. 534:69–77.

Singh BK, Walker A. 2006. Microbial degradation of organophosphorus compounds. FEMS Microbiol Rev. 30:428–471.

Sogorb MA, Vilanova E. 2002. Enzymes involved in the detoxification of organophosphorus, carbamate and pyrethroid insecticides through hydrolysis. Toxicol Lett. 128:215–228.

Tang X, Liang B, Yi T, Manco G, Liu A. 2014. Cell surface display of organophosphorus hydrolase for sensitive spectrophotometric detection of p-nitrophenol substituted organophosphates. Enzyme Microb Technol. 55:107–112.

Tang X, Zhang T, Liang B, Han D, Zeng L, Zheng C, Li T, Wei M, Liu A. 2014. Sensitive electrochemical microbial biosensor for p-nitrophenylorganophosphates based on electrode modified with cell surface-displayed organophosphorus hydrolase and ordered mesopore carbons. Biosens Bioelectron. 60:137–142.

Thakur S, Kumar P, Reddy MV, Siddavattam D, Paul A. 2013. Enhancement in sensitivity of fluorescence based assay for organophosphates detection by silica coated silver nanoparticles using organophosphate hydrolase. Sens Actuators B Chem. 178:458–464.

Theriot CM, Grunden AM. 2011. Hydrolysis of organophosphorus compounds by microbial enzymes. Appl Microbiol Biotechnol. 89:35–43.

Tokuriki N, Tawfik DS. 2009. Chaperonin overexpression promotes genetic variation and enzyme evolution. Nature. 459:668.

Trojanowicz M, Mulchandani A, Mascini M. 2004. Carbon nanotubes-modified screen-printed electrodes for chemical sensors and biosensors. Anal Lett. 37:3185–3204.

Vilanova E, Sogorb MA. 1999. The role of phosphotriesterases in the detoxication of organophosphorus compounds. Crit Rev Toxicol. 29: 21–57.

Vyas NK, Nickitenko A, Rastogi VK, Shah SS, Quiocho FA. 2010. Structural insights into the dual activities of the nerve agent degrading organophosphate anhydrolase/prolidase. Biochemistry. 49:547–559.

Wagner SL, Orwick DL. 1994. Chronic organophosphate exposure associated with transient hypertonia in an infant. Pediatrics. 94:94–97.

Wales ME, Reeves TE. 2012. Organophosphorus hydrolase as an in vivo catalytic nerve agent bioscavenger. Drug Test Anal. 4:271–281.

Walker JP, Kimble KW, Asher SA. 2007. Photonic crystal sensor for organophosphate nerve agents utilizing the organophosphorus hydrolase enzyme. Anal Bioanal Chem. 389:2115–2124.

Wang J, Chen L, Mulchandani A, Mulchandani P, Chen W. 1999. Remote biosensor for in-situ monitoring of organophosphate nerve agents. Electroanalysis. 11:866–869.

Wang J, Krause R, Block K, Musameh M, Mulchandani A, Mulchandani P, Chen W, Schöning MJ. 2002. Dual amperometric–potentiometric biosensor detection system for monitoring organophosphorus neurotoxins. Anal Chim Acta. 469:197–203.

Wang J, Krause R, Block K, Musameh M, Mulchandani A, Schöning MJ. 2003. Flow injection amperometric detection of OP nerve agents based on an organophosphorus–hydrolase biosensor detector. Biosens Bioelectron. 18:255–260.

White BJ, Harmon HJ. 2005. Optical solid-state detection of organophosphates using organophosphorus hydrolase. Biosens Bioelectron. 20: 1977–1983.

Yoshimoto T, Tone H, Honda T, Osatomi R, Kobayashi R, Tsuru D. 1989. Sequencing and high expression of aminopeptidase P gene from *Escherichia coli* HB101. J Biochem. 105:412–416.

Zhang X. 2004. Real time and in vivo monitoring of nitric oxide by electrochemical sensors—from dream to reality. Front Biosci. 9:3434.

Zheng J, Constantine CA, Zhao L, Rastogi VK, Cheng TC, DeFrank JJ, Leblanc RM. 2005. Molecular interaction between organophosphorus acid anhydrolase and diisopropylfluorophosphate. Biomacromolecules. 6:1555–1560.

Zimmer LA, Ennis M, Wiley RG, Shipley MT. 1998. Nerve gas-induced seizures: role of acetylcholine in the rapid induction of Fos and glial fibrillary acidic protein in piriform cortex. J Neurosci. 18: 3897–3908.

Zourob M, Ong KG, Zeng K, Mouffouk F, Grimes CA. 2007. A wireless magnetoelastic biosensor for the direct detection of organophosphorus pesticides. Analyst. 132:338–343.

Zourob M, Simonian A, Wild J, Mohr S, Fan X, Abdulhalim I, Goddard N. 2007. Optical leaky waveguide biosensors for the detection of organophosphorus pesticides. Analyst. 132:114–120.